A numerical-tensorial "hybrid" nuclear motion Hamiltonian and dipole moment operator for spectra calculation of polyatomic nonrigid molecules

Michael M. Rey, Dominika Viglaska, Oleg Egorov, Andrei Nikitin

A numerical−tensorial "hybrid" nuclear motion Hamiltonian and dipole moment operator for spectra calculation of polyatomic nonrigid molecules

Michaël Rey,[1, a)] Dominika Viglaska,[1] Oleg Egorov,[2, 3] and Andrei V. Nikitin[2]

[1)] *Groupe de Spectrométrie Moléculaire et Atmosphérique, UMR CNRS 7331, BP 1039, F-51687, Reims Cedex 2, France*

[2)] *Laboratory of Theoretical Spectroscopy, V.E. Zuev Institute of Atmospheric Optics SB RAS 1, Akademician Zuev Sq., Tomsk, 634055 Russia*

[3)] *Tomsk State University 36, Lenin Ave., Tomsk, 634050 Russia*

(Dated: 25 August 2023)

The analysis and modelling of high-resolution spectra of nonrigid molecules require a specific Hamiltonian and group-theoretical formulation which differs significantly from that of more familiar rigid systems. Within the framework of the Hougen-Bunker-Johns (HBJ) theory, this paper is devoted to the construction of a nonrigid Hamiltonian based on a suitable combination of numerical calculations for the nonrigid part in conjunction with the irreducible tensor operator method for the rigid part. For the first time, a variational calculation from *ab initio* potential energy surfaces is performed using the HBJ kinetic energy operator build from vibrational, large-amplitude motion and rotational tensor operators expressed in terms of curvilinear and normal coordinates. Group theory for nonrigid molecules plays a central role in the characterization of the overall tunnelling splittings and is discussed in the present approach. The construction of the dipole moment operator is also examined. Validation tests consisting in a careful convergence study of the energy levels as well as in a comparison of results obtained from independent computer codes are given for the nonrigid molecules CH_2, CH_3, NH_3 and H_2O_2. This work paves the way for the modelling of high-resolution spectra of larger nonrigid systems.

Keywords: Nonrigid molecules, tensorial formalism, numerical-algebraic calculation.

[a)] Electronic mail: michael.rey@univ-reims.fr

I. INTRODUCTION

Vibration-rotation spectroscopy remains a formidable tool to understand spectral features of known molecules or to identify "unknown" molecules in astrophysics, either from laboratory experimental spectra or from accurate theoretical calculations[1,2]. The standard and historical way of interpreting high-resolution molecular spectra consists in using empirical effective Hamiltonians suitable for data fitting[3–6]. In turn, it may arise that some resulting fitted parameters have a limited extrapolation power. With the increase in computing capability, particular effort was made these past two decades in nuclear-motion theory to obtain variational eigenpairs relying on the development of efficient and optimized methods for solving the time-independent Schrödinger equation[7–35]. Within this context, the derivation of exact quantum kinetic energy operators (KEO) from different coordinate systems as well as the construction of highly accurate *ab initio* potential energy surfaces (PES) remain an active field of research[36–49]. For semirigid molecules whose PES has a single, well-defined equilibrium configuration, the use of normal coordinates within the framework of the Eckart-Watson Hamiltonian formalism[50] is well established. Recent papers[23,51–55] devoted to the construction of accurate line lists for many polyatomic semirigid molecules proved how the Watson Hamiltonian was still of primary importance for the modelling of planetary atmospheres. For nonrigid "floppy" molecules exhibiting one or several large amplitude motions (LAM) connecting multiple potential wells, the use of rectilinear normal coordinates designed for small amplitude vibrations is clearly prohibited. General internal-coordinate Hamiltonians[19,39,40,47,56–61] were thus constructed in order to study the complex intra-molecular dynamics arising from inversion or internal rotational motions. Indeed, the study of molecules undergoing LAMs is particularly challenging because of their dense and rich spectra due to numerous tunnelling splittings[62–65]. With the spectacular advances in modern experimental techniques, even small splittings can be now resolved, making necessary the development of sophisticated theoretical models to analyse spectra.

Though it does not give any information about the magnitude of the splittings, group theory plays a central role[66–72] and is inseparable from the theory of the nonrigid molecules. It helps to characterize all the tunnelling splitting patterns and to provide meaningful labels to the vibration-LAM-rotation states. But in the absence of a unique equilibrium geometry, it is of course obvious that the irreducible representations (irreps) of standard point

groups cannot be used to properly label the wave functions of molecules with observable tunnelling[62,67,68,70,73]. Instead, the wave functions of a nonrigid molecule can be classified under the complete nuclear permutation inversion (CNPI) groups[66,74]. However, when the number of permutation and permutation-inversion elements grows, the use of CNPI becomes rapidly awkward. To avoid manipulating symmetry species associated with tunnelling splitting that will be never resolved, it is thus convenient to select only "feasible" operations that bring the molecule into attainable geometries. All these elements form a molecular symmetry (MS) group[74] which can be seen as the point group counterpart for floppy molecules and whose irreps help to classify unambiguously the molecular states.

Undoubtedly, the curvilinear coordinates are the best choice to describe LAMs but we can wonder what kind of coordinates can be used to describe the small amplitude vibrations. In 1970, Hougen, Bunker and Johns[75,76] (HBJ) derived an exact kinetic energy operator for nonrigid molecules, based on a clever combination of normal coordinates for the "rigid" vibrations and of curvilinear coordinates for the LAM(s). The other major difference with the standard treatment of rigid molecules lies in the fact that the equilibrium configuration is now replaced by a so-called nonrigid reference configuration depending on the LAM coordinate(s). These past four decades, the HBJ Hamiltonian led to the construction of different types of effective Hamiltonians[77–86], using different types of approximations, after applying contact transformation perturbation theory to account for the effects of the small vibrations (more references as well as a non-exhaustive list of computer programs can be found Section III and Tab. 1 of Ref.[87]). To our knowledge, the HBJ Hamiltonian using a KEO expressed in terms of normal coordinates was never used in a full variational calculation to compute vibration-rotation spectra from *ab initio* PESs. Instead, other models also based on the HBJ philosophy and using a KEO expanded in terms of valence or Morse-like coordinates were developed and implemented in the MORBID[56] and TROVE[57] computer codes.

The aim of this paper is to provide a complete nuclear motion normal-mode HBJ-based Hamiltonian where the LAM coordinate is defined on a grid, combined with advanced group-theoretical methods and optimization tools for solving the Schrödinger equation. The rigid part of the Hamiltonian is treated algebraically with the aid of irreducible tensor operators (ITO) while the LAM coordinate is treated numerically. A so-called *hybrid* model is thus proposed for the first time. Note that another hybrid model was developed in Ref.[86], but not in that same context. The computation of the vibration-LAM-rotation energy levels is

performed variationally using symmetry-adapted primitive basis functions. The construction of a hybrid dipole moment operator is also discussed for line intensity calculation. These past few years, a set of optimized reduction-compression tools was developed to make variational calculations as tractable as possible for semirigid molecules (see *e.g.* Refs.[13,88–90]), so that at this stage a simple question is raised: *Can the hybrid model benefit from already existing reduction and symmetry tools initially designed for semirigid molecules?* We will try to respond this question along this paper, helped by a series of validation tests and illustrative examples.

In this paper, we will focus on molecules with only one LAM, like inversion or internal rotation, although the extension to several LAMs would be of course feasible. The next section recalls the main recipe as well as the basic ingredients which are useful in the HBJ theory, in particular around the choice of the molecule-fixed frame as well as coordinate transformations to conveniently rewrite the potential part. Section III first explains why the HBJ theory is relevant, related to what was previously developed for semirigid molecules. Then a normally-ordered form of the HBJ KEO will be proposed before focusing on symmetry considerations. The construction of the "numerical-ITO" hybrid Hamiltonian and dipole moment operator will be presented and the choice of the grid points will be also discussed during the computation of the matrix elements. The validation of the present model will be given in Section IV which will also provide a careful examination of the convergence of the energy levels for four nonrigid molecules: CH_2, CH_3, NH_3 and H_2O_2.

II. TREATMENT OF A MOLECULE EXHIBITING A LARGE AMPLITUDE MOTION: PRELIMINARIES

A. Nonrigid reference configuration and choice of the molecule-fixed axis system

In the standard treatment of semirigid molecules, the vibrational displacements of the atomic nuclei are measured with respect to a rigid, equilibrium geometry configuration $\mathbf{a}_i^e$ ($i = 1, \cdots, N$), with N the number of atoms, and in that case both the reciprocal $\mu_{\alpha\beta}$ tensor contained in the KEO as well as the potential V are well approximated by the leading terms in a Taylor series expansion. For nonrigid molecules for which the amplitude of at least

one coordinate is not small compared to the equilibrium bond lengths and bond angles, the representation of $\mu_{\alpha\beta}$ and V as a Taylor series fails. Thus, the potential function for the LAM cannot be properly described, even by increasing the order of the polynomial expansion. In order to prevent from such dramatic convergence issues, Hougen, Bunker and Johns[75], in their seminal work on quasilinear triatomic molecules, suggested to remove the bending motion from the vibrational part and to incorporate this LAM into the rotational part. To this end, they (i) introduced a so-called nonrigid reference configuration $\mathbf{a}_i^{\text{ref}}(\rho)$ instead of $\mathbf{a}_i^e$ where ρ is a coordinate describing the LAM and (ii) treated the remaining $3N-7$ small amplitude vibrations using the normal mode coordinates on a numerical grid in ρ. By definition, the displacements of the coordinates describing the small amplitude motions are assumed zero along the reference configuration. The HBJ approach thus ensures that these $3N-7$ coordinates vary smoothly around $\mathbf{a}_i^{\text{ref}}(\rho)$, making relevant a Taylor series expansion of both the KEO and V in terms of normal coordinates.

Though initially developed for quasilinear triatomic molecules, the HBJ approach can be finally applied to a wide class of nonrigid polyatomic molecules exhibiting different kind of LAM (bending, inversion or internal rotation). The major difference between the HBJ Hamiltonian[75] and its rigid counterpart, namely the Eckart-Watson Hamiltonian[50], lies in the fact that all the coefficients involved in the KEO and in the Taylor expansion of the potential part will be now ρ dependent (see Sections II B & III B).

At this stage, we need to choose the orientation of the molecule-fixed axis system for the reference configuration. As usual, its origin will be placed at the center of mass. For semirigid molecules, the frame is generally oriented to coincide with the principal axis system at the equilibrium geometry. For nonrigid molecules, several choices arise. Among the possibilities, the principal axis system (PAS), rho axis system (RAS) or internal axis system (IAS) can be considered to vanish some coupling terms in the generalized inertia matrix $\mathbf{I}^{\text{ref}}$ when all the displacements $\mathbf{d}_i$ are zero (see *e.g.* the discussion of Flaud & Perrin in Ref.[91]). The PAS allows to remove the inertial cross terms $I_{\alpha\beta}^{\text{ref}}$. In order to minimize the rotation-LAM coupling by removing the cross terms $I_{\alpha\rho}^{\text{ref}}$ $(\alpha = x, y, z)$ in $\mathbf{I}^{\text{ref}}$, IAS is good choice. Mathematically speaking, this latter condition implies to vanish the angular-momentum-like vector due to ρ

$$\sum_{i=1}^{N} m_i \mathbf{a}_i^{\text{ref,IAS}}(\rho) \times \frac{d\mathbf{a}_i^{\text{ref,IAS}}(\rho)}{d\rho} = \mathbf{0}, \tag{1}$$

with $\mathbf{a}_i^{\mathrm{ref,IAS}}(\rho) = \mathbf{U}(\rho)\mathbf{a}_i^{\mathrm{ref,MF_1}}(\rho)$ and $\sum_i m_i \mathbf{a}_i^{\mathrm{ref,IAS}}(\rho) = 0$. Here $\mathbf{a}_i^{\mathrm{ref,MF_1}}(\rho)$ is the reference configuration in some arbitrary reference axis system $\mathrm{MF_1}$ and $\mathbf{U}(\rho)$ a ρ-dependent rotation matrix to be determined. This choice is analogous to the original HBJ axis system for triatomic molecules[75], followed soon after by a series of works where an auxiliary angle[79,81,92] $\epsilon(\rho)$ satisfying Eq. (1) was introduced instead of $\mathbf{U}(\rho)$. A recent method was proposed in Ref.[93] for the derivation of the rotation matrix $\mathbf{U}(\rho)$ and is briefly recalled in Appendix. In the RAS, the angular momentum due to the LAM is not vanishing but is of constant magnitude along the z axis[6].

As an illustrative example, we have determined the rotation matrix $\mathbf{U}(\rho)$ in order to compute a new reference configuration satisfying (1) for the H_2O_2 molecule. As a starting point, we have considered the reference configuration given in Ref.[94], called $\mathbf{a}_i^{\mathrm{ref,ini}}(\rho)$ such as $I_{y\rho} \neq 0$. By solving Eq. (A6), the new IAS configuration is given by $\mathbf{a}_i^{\mathrm{ref,IAS}}(\rho) = \mathbf{U}(\rho)\mathbf{a}_i^{\mathrm{ref,ini}}(\rho)$. The x components of the reference configuration for the atoms H1 and O1, before and after transformation, are displayed in Fig. 1 as a function of ρ. It is worth mentioning that within the IAS treatment the torsion angle ρ will be defined as half of the dihedral angle when studying internal rotation. As a direct consequence, the rotational and torsion angles, χ and ρ, will be double valued, making necessary the use of irreps of extended MS groups to classify the rotational and torsional energy levels.

Moreover, according to the relation between the laboratory and molecule-fixed axis systems, it turns out that the infinitesimal vibrational displacement vectors $\mathbf{d}_i$ must be subjected to 7 constrains. There are 3 equations corresponding to the center of mass condition, 3 other ones have a form similar to the Eckart conditions and a last one (the Sayvetz condition[95]) minimizing the interaction between the small and large amplitude vibrations.

B. Coordinate transformation and expansion of the potential energy surface

In the previous section, the LAM coordinate ρ as well as the notion of reference configuration attached to a molecule-fixed axis system have been introduced. As stated by Jensen and Szalay[81,96,97], ρ can be considered as a kind of "effective" coordinate which is different from the geometrically defined curvilinear $\bar{\rho}$ coordinate when the "rigid" vibrations are beyond their equilibrium geometry. By construction, the HBJ KEO depends explicitly on ρ and on $3N-7$ rectilinear, normal coordinates Q_i while the *ab initio* potential function is built

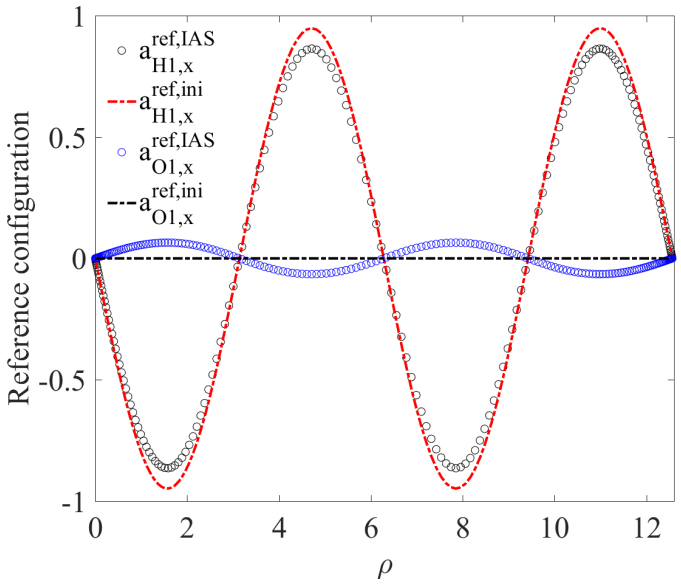

FIG. 1. Plot of the x components of the reference configuration as a function of ρ (in radian) for the atoms H1 and O1 of H_2O_2 in the initial axis system ($I_{y\rho} \neq 0$) and in the final IAS ($I_{y\rho} = 0$) computed from the transformation $\mathbf{U}(\rho)$ obtained by solving Eq. (A6).

from a function $\bar{u}(\bar{\rho})$ where $\bar{\rho}$ describes a bond, torsion or inversion angle, and from a set of curvilinear coordinates (*i.e.* valence, Morse, cosine, etc.) to describe the small amplitude vibrations. In this work, we assume that the potential function V is known and expressed in terms of $3N-6$ coordinates $S^{(\Gamma_k)}_{k,\sigma_k}$ adapted to the symmetry of the molecule, where Γ_k is an irreducible representation of a molecular symmetry group and σ_k a component when $dim(\Gamma_k) > 1$. Among these $S^{(\Gamma_k)}_{k,\sigma_k}$ coordinates, one corresponds to $\bar{u}(\bar{\rho})$ and needs to be transformed to a ρ-dependent function to be consistent with the KEO. To this end, it is more convenient to rewrite the PES in terms of the $3N-7$ coordinates $S^{(\Gamma_r)}_{r,\sigma_r}$ for the rigid part and put the dependence in $\bar{\rho}$ into the expansion coefficients. As a direct consequence, some linear terms $\sum_r \bar{F}_r(\bar{\rho}) S^{(\Gamma_r)}_r$ will now appear in the potential while the quadratic part will be written as $\sum_r \bar{F}_{r,r'}(\bar{\rho}) S^{(\Gamma_r)}_r S^{(\Gamma'_{r'})}_{r'}$. Thus, contrary to the "ordinary" treatment of semirigid molecules, vibrations with different symmetries can interact in the quadratic part of the potential for nonrigid molecules.

In order to solve the GF problem, we first need to express the PES as a function of the ρ coordinate, instead of $\bar{\rho}$. To this end, a general numerical recipe was proposed in Ref.[87] to find the relation $\bar{\rho} = f(\rho, S_r)$ for any polyatomic molecules, so that the potential function

transforms as $V(S_r, \bar{\rho}) \rightarrow V(S_r, \rho)$. The procedure can be summarized as follows.

– First, we assume that all calculations are performed on a grid composed of M_ρ points

$$\rho_m \in [\rho_{min}, \rho_{max}],\ m = 1, \cdots, M_\rho, \tag{2}$$

where the choice of these points will be discussed in Section III C 4. As already mentioned, the main drawback of the HBJ approach lies in the fact that the kinematic matrix of dimension $(3N-7)\times(3N-7)$ writes as $\mathbf{G} = \mathbf{G}(\rho_m)$ due to its dependence to $a_{i\alpha}^{\rm ref}(\rho)$ whereas the elements of the force constant matrix write $\bar{F}_{rr'} = \bar{F}_{rr'}(\bar{\rho})$. The aim is thus to find the transformation $\bar{\mathbf{F}}(\bar{\rho}) \rightarrow \mathbf{F}(\rho_m)$ to properly solve the GF problem on the grid. To this end, we have shown in Ref.[87] that $\bar{u}(\bar{\rho})$ must be necessarily of the form

$$\bar{u}(\bar{\rho}) = u(\rho_m) + \sum_r C_r(\rho_m) S_r^{(\Gamma_r)} + \sum_{rr'} C_{rr'}(\rho_m) S_r^{(\Gamma_r)} S_{r'}^{(\Gamma_{r'})}, \tag{3}$$

where the C_r and $C_{rr'}$ coefficients are to be determined. In this approach, only the linear and quadratic terms are needed, unlike the MORBID approach where higher-order expansion coefficients $C_{rr'r''}$, $C_{rr'r''r'''}$, *etc.*, were required[56].

– In the next step, we expand the $3N-7$ coordinates $S_r^{(\Gamma_r)}$ as well as the seven Eckart-Sayvetz relations

$$\begin{aligned}
\mathcal{T}_\alpha &= \frac{1}{\sqrt{M}} \sum_i m_i d_{i\alpha}, \\
\mathcal{R}_\alpha &= \frac{1}{\sqrt{I_{\alpha\alpha}^{\rm ref}(\rho)}} \sum_i m_i \epsilon_{\alpha\beta\gamma} a_{i\beta}^{\rm ref}(\rho) d_{i\gamma}, \\
\mathcal{S} &= \frac{1}{\sqrt{I_{\rho\rho}^{\rm ref}(\rho)}} \sum_{i,\alpha} m_i \frac{da_{i\alpha}^{\rm ref}(\rho)}{d\rho} d_{i\alpha},
\end{aligned} \tag{4}$$

in terms of the $3N$ small amplitude Cartesian displacements $\mathbf{d}_i$. Here, M is the total mass of the system, ϵ corresponds to the Levi-Civita tensor and $I_{\alpha\alpha}^{\rm ref}$, $I_{\rho\rho}^{\rm ref}$ are the diagonal elements of the 4×4 inertia matrix[75]. In the standard treatment of semirigid molecules, only the linearized part $\mathbf{S} = \mathbf{B}\mathbf{d}$ is required for solving the GF problem, but here we also need to compute the quadratic terms $\mathbf{d}_i\mathbf{d}_j$ to determine the C_r and $C_{rr'}$ coefficients in Eq. (3). To this end, we first construct the $3N$ linear and $3N(3N+1)/2$ quadratic forms X_s^{lin} and $X_{s''}^{quad} = X_s^{lin} X_{s'}^{lin}$ $(s, s' = 1, \cdots, 3N,\ s \geq s';\ s'' = 1, \cdots, 3N(3N+1)/2)$ with $\mathbf{X}^{lin} = (\mathbf{S}, \mathcal{T}_\alpha, \mathcal{R}_\alpha, \mathcal{S})$. Similarly, we define the vector $\mathbf{Y}^{lin} = (d_{1x}, \cdots, d_{Nz})$ and also construct the quadratic forms $Y_{s''}^{quad} = Y_s Y_{s'}$. Finally, we follow closely the strategy established in Ref.[98] to make this problem linear by defining the transformation $\mathbf{B}_{quad}$ on the grid such that

$$(\mathbf{X}^{lin}, \mathbf{X}^{quad})^t = \mathbf{B}_{quad}(\rho_m)\ \ (\mathbf{Y}^{lin}, \mathbf{Y}^{quad})^t. \tag{5}$$

The Cartesian displacements contained in $\mathbf{Y}$ can be thus deduced by inverting Eq. (5) and by using the seven constrains $\mathcal{T}_\alpha = \mathcal{R}_\alpha = \mathcal{S} = 0$. We thus write

$$(\mathbf{d}_1, \cdots, \mathbf{d}_N)^t = \mathbf{A}^{inv}_{quad}(\rho_m)\ (\mathbf{X}^{lin}, \mathbf{X}^{quad})^t, \tag{6}$$

with now $\mathbf{X}^{lin} = (\mathbf{S}, 0, 0, 0)$ and where $\mathbf{A}^{inv}_{quad}$ is a sub-matrix extracted from $\mathbf{B}^{-1}_{quad}$. In this scheme, the nuclear displacement vectors $\mathbf{d}_i$ are variables depending on both the symmetry and ρ coordinates.

– In the last step, we express the function $\bar{u}(\bar{\rho})$ in terms of Cartesian coordinates and make the substitution (6) to finally get the desired coefficients C_r and $C_{rr'}$ in Eq. (3). We are now able to find the eigensolutions of the **GF** matrix and convert the *ab initio* curvilinear potential function to a normal-mode polynomial expansion for each ρ_m

$$V(S_r, \bar{\rho}) \rightarrow V(Q_r, \rho_m) \equiv V_{\rho_m}(Q_r),\ r = 1, \cdots, 3N-7, \tag{7}$$

using Eq. (3) as well as the $3N \times (3N-7)$ orthogonal transformation $\mathbf{l}(\rho_m)$ linking the mass-weighted Cartesian displacements to the normal coordinates[99].

In Ref.[87], we intended at this stage to fit all the matrix elements $l_{i\alpha,s}(\rho_m)$ as well as all the Coriolis coefficients $\zeta^{\alpha}_{ss'}(\rho_m)$ to a polynomial function in $u(\rho)$ in order to expand both the KEO and potential parts in terms of the $3N-6$ coordinates (Q_i, ρ), like for semirigid molecules. In this work, the nonrigid part of the HBJ Hamiltonian will be treated numerically for more flexibility, which is the best choice if certain values of ρ are near a singularity.

III. CONSTRUCTION OF A HYBRID HBJ-BASED MODEL

A. Motivations

These past years, a general methodology based on the normal-mode Eckart-Watson formalism and on the extensive use of symmetry was proposed for semirigid molecules. It also combines dimensionality reduction techniques to manage memory at each stage of calculation. All the procedure has been implemented in the TENSOR computer code and led to the construction of accurate line lists for molecules up to seven atoms[13,21,51–53]. The main motivations for the extension to nonrigid systems can be summarized as follows:

1 – Reduction-compression techniques. The use of the HBJ theory is a quite natural choice

because most of the reduction-compression tools previously developed for semirigid molecules can be also considered and adapted to tackle the problem of nonrigid polyatomic molecules.
2 − A general formulation. Like for the Watson KEO, the form of the HBJ KEO remains the same whatever the number of atoms. Moreover, the use of the ρ coordinate allows an optimal separation between small and large amplitude nuclear motions, achieved by the Sayvetz condition.
3 − Variational calculation. The HBJ model inspired a series of works and led to the development of both effective vibration-LAM-rotation Hamiltonians suitable for data fitting[77–86] and nuclear-motion Hamiltonians, as those implemented in the MORBID[56] and TROVE[57] computer codes. In this work, we intend using the HBJ Hamiltonian in its original formulation based on the 3N-7 normal coordinates, including all terms in Eqs. (10)-(14) below, for solving variationally the vibration-LAM-rotation wave equation.
4 − Extensive use of symmetry. HBJ should also benefit from the use of the ITO formalism for a full account of symmetry properties. The use of ITOs is probably the best efficient way for dealing with degenerate vibrations when the molecular symmetry group is non-Abelian. The suitable combination of ITOs with a numerical treatment of the LAM will lead to the introduction of a so-called *hybrid* Hamiltonian model for the spectra calculation of nonrigid molecules.
5 − Towards a nonrigid effective model. Effective Hamiltonian computer codes designed to calculate and fit energy levels and line transitions for molecules containing one or several internal rotors already exist and were developed these past three decades (see *e.g.* the XIAM[100], BELGI-C_1[101], BELGI-C_s[102], BELGI-C_s-2Tops[103], ERHAM[104] or RAM36[85] codes). Recently, we have proposed a numerical approach for the construction of *ab initio* effective models[90] which is a clear alternative to the rather involved Van Vleck perturbation method. Undoubtedly, this approach could be of great help to extract effective nonrigid Hamiltonian from our hybrid model and to refine parameters on the experimental data, even when several interacting vibrational states are involved.

B. Expansion of the HBJ kinetic energy operator

We have shown in the previous section how the *ab initio* potential energy function V in Eq. (7) can be expanded on a numerical grid in terms of $3N-7$ normal coordinates Q.

The KEO can be also expressed as a sum of products in the same fashion. In that case, each integral is a product of integrals associated with each mode and the computation of the matrix elements can benefit from the use of the Wigner-Eckart theorem (see Section III C 4). In this work, we propose to put each term of the expansion into a better suited normally-ordered form of the type $X(Q)Y(P)Z(J_\alpha)$ where X and Y are not necessarily commuting functions. Such a form is quite convenient to build the KEO at any order and in a systematic manner. Unless specified otherwise, the running indices j, k, l, r and s will take values $1,\cdots,3N-7$ while the Greek letters α and β will equal x, y, z or ρ. We can show that the HBJ KEO can be rewritten for each point ρ_m of the grid as

$$\begin{aligned} 2T^{HBJ}_{\rho_m} &= \sum_{jl} f_{jl}(\mathbf{Q},\rho_m)P_jP_l + \sum_{l} g_{l}(\mathbf{Q},\rho_m)P_l \\ &+ \sum_{l\beta} t_{l\beta}(\mathbf{Q},\rho_m)P_lJ_\beta + \sum_{\beta} h_{\beta}(\mathbf{Q},\rho_m)J_\beta \\ &+ \sum_{\alpha\beta} \mu_{\alpha\beta}(\mathbf{Q},\rho_m)J_\alpha J_\beta + W(\mathbf{Q},\rho_m), \end{aligned} \tag{8}$$

with the corresponding volume element of integration

$$d\tau = \sin\theta d\theta d\phi d\chi d\rho dQ_1 dQ_2 \cdots dQ_{3N-7}. \tag{9}$$

Here, $P_j = -i\hbar\partial/\partial Q_j$ is the conjugate momentum of the normal coordinates Q_j while J_α ($\alpha = x, y, z$) and $J_\rho = -i\hbar d/d\rho$ are the components of the total angular momentum and LAM coordinate, respectively. If $\alpha \neq \beta$, the terms containing $J_\alpha J_\beta$ are sorted as J_xJ_y, J_xJ_z and J_yJ_z. For the sake of simplicity, the symmetry labels have been omitted in all the coordinates and conjugate momenta that are simply denoted here by $Q^{(\Gamma)}_{k\sigma} \equiv Q_j$, $J^{(\Gamma)}_{\rho} \equiv J_\rho$, etc. To be rigorous, these symmetry labels should appear everywhere and in that case the k index in $Q^{(\Gamma)}_{k\sigma}$ would run over the vibrational modes instead of the vibrational coordinates.

Each term in Eq. (8) is a polynomial function in $(Q_i, P_i, J_\rho, J_\alpha)$ and is computed for each ρ_m, like for the potential part. Using the well-known commutation rules and after some algebra, it is straightforward to show that

$$f_{jl}(\mathbf{Q},\rho_m) = \sum_{rk\alpha\beta} \zeta^{\alpha}_{rj}(\rho_m)\zeta^{\beta}_{kl}(\rho_m)Q_rQ_k\mu_{\alpha\beta} + \delta_{jl}, \tag{10}$$

$$
\begin{aligned}
g_l(\mathbf{Q},\rho_m) = & -i\hbar \sum_{rsk\alpha\beta} \left\{ \zeta^{\alpha}_{rs}\zeta^{\beta}_{kl} Q_r Q_k \frac{\partial \mu_{\alpha\beta}}{\partial Q_s} - \frac{1}{4}\zeta^{\alpha}_{rs}\zeta^{\beta}_{kl} Q_r Q_k \mu_{\alpha\beta} \frac{\partial \ln\mu}{\partial Q_s} \right. \\
& \left. + \zeta^{\alpha}_{rs}\zeta^{\beta}_{kl} Q_r \mu_{\alpha\beta}\delta_{ks} + \frac{1}{4}\zeta^{\alpha}_{rl}\zeta^{\beta}_{ks} Q_r Q_k \mu_{\alpha\beta} \frac{\partial \ln\mu}{\partial Q_s} \right\} \\
& + i\hbar \sum_{r\alpha} \zeta^{\alpha}_{rl} Q_r \frac{d\mu_{\alpha\rho}}{d\rho} + i\hbar \sum_{r\alpha} \frac{d\zeta^{\alpha}_{rl}}{d\rho} Q_r \mu_{\alpha\rho},
\end{aligned}
\tag{11}
$$

$$
t_{l\beta}(\mathbf{Q},\rho_m) = -2 \sum_{r\alpha} \zeta^{\alpha}_{rl} Q_r \mu_{\alpha\beta}
\tag{12}
$$

$$
h_{\beta}(\mathbf{Q},\rho_m) = -i\hbar \frac{d\mu_{\beta\rho}}{d\rho} + i\hbar \sum_{rs\alpha} \zeta^{\alpha}_{rs} Q_r \frac{\partial \mu_{\alpha\beta}}{\partial Q_s},
\tag{13}
$$

and with the pseudo-potential

$$
\begin{aligned}
W(\mathbf{Q},\rho_m) = & \frac{\hbar^2}{16} \sum_r \left(\frac{\partial \ln\mu}{\partial Q_r} \right)^2 - \frac{\hbar^2}{4} \sum_r \frac{\partial^2 \ln\mu}{\partial Q_r^2} - \frac{\hbar^2}{4} \left(\frac{d\mu_{\rho\rho}}{d\rho} \right) \left(\frac{d\ln\mu}{d\rho} \right) \\
& + \frac{\hbar^2}{16} \mu_{\rho\rho} \left(\frac{d\ln\mu}{d\rho} \right)^2 - \frac{\hbar^2}{4} \mu_{\rho\rho} \left(\frac{d^2\ln\mu}{d\rho^2} \right) + \frac{\hbar^2}{4} \sum_{rs\alpha} \mu_{\alpha\rho} \left(\frac{d\zeta^{\alpha}_{rs}}{d\rho} \right) \left(\frac{\partial \ln\mu}{\partial Q_s} \right) \\
& + \frac{\hbar^2}{4} \sum_{rs\alpha} \zeta^{\alpha}_{rs} Q_r \left\{ \left(\frac{d\mu_{\alpha\rho}}{d\rho} \right) \left(\frac{\partial \ln\mu}{\partial Q_s} \right) - \frac{1}{2} \mu_{\alpha\rho} \left(\frac{d\ln\mu}{d\rho} \right) \left(\frac{\partial \ln\mu}{\partial Q_s} \right) \right. \\
& \left. + 2\mu_{\alpha\rho} \frac{d}{d\rho} \left(\frac{\partial \ln\mu}{\partial Q_s} \right) + \left(\frac{\partial \mu_{\alpha\rho}}{\partial Q_s} \right) \left(\frac{d\ln\mu}{d\rho} \right) \right\} \\
& - \frac{\hbar^2}{4} \sum_{rskl\alpha\beta} \zeta^{\alpha}_{rs}\zeta^{\beta}_{kl} \left\{ Q_r Q_k \left(\frac{d\mu_{\alpha\beta}}{dQ_s} \right) \left(\frac{\partial \ln\mu}{\partial Q_l} \right) - \frac{1}{4} Q_r Q_k \mu_{\alpha\beta} \left(\frac{\partial \ln\mu}{\partial Q_s} \right) \left(\frac{\partial \ln\mu}{\partial Q_l} \right) \right. \\
& \left. + Q_r \mu_{\alpha\beta} \left(\frac{\partial \ln\mu}{\partial Q_l} \right) \delta_{ks} + Q_r Q_k \mu_{\alpha\beta} \left(\frac{\partial^2 \ln\mu}{\partial Q_s \partial Q_l} \right) \right\},
\end{aligned}
\tag{14}
$$

where μ is the determinant of the 4×4 reciprocal inertia matrix with the components $\mu_{\alpha\beta}$ computed from the inverse of $I'_{\alpha\beta}$ (see *e.g.* Refs.[75,81] for all the definitions and for the expression of the Coriolis coefficients ζ). The various quantities involved in Eqs. (10)-(14) are also evaluated for each ρ_m, that is $\mu_{\alpha\beta} = \mu_{\alpha\beta}(\mathbf{Q},\rho_m)$, $\zeta = \zeta(\rho_m)$, $\mu'_{\alpha\beta} = \mu'_{\alpha\beta}(\mathbf{Q},\rho_m)$ or $(\ln\mu)' = (\ln\mu)'(\mathbf{Q},\rho_m)$.

The expression (8) of the normally-ordered HBJ KEO as well as the numerical procedure in Section II have been implemented in an updated version of our TENSOR computer code. In order to find the Taylor series of (7) and (8) in terms of the $3N-7$ normal coordinates, the crucial point is the computation of the successive derivatives.

– The first and second derivatives in ρ involved in (8) are evaluated numerically using the 5-points central finite difference formula and quadruple-precision floating-point numbers.

– To circumvent the problem of round-off errors encountered in the finite difference method for high-order derivatives with respect to the $3N-7$ normal coordinates, a modified version of the computer program COSY Infinity[105], including now the dynamic allocation and the quadruple precision, was implemented in the TENSOR code. It allows a high-order multivariate automatic differentiation without almost no loss of precision. The Taylor series expansions of V, $\mu_{\alpha\beta}$, $\ln\mu$ and their derivatives with respect to Q_i and ρ are thus all performed using the COSY algorithm. The mixed derivative $d(\frac{\partial \ln\mu}{\partial Q_s})/d\rho$ involved in (14) combines finite difference and COSY calculation. The convergence of both the KEO and potential parts will be discussed in Section IV in the case of 3- and 4-atomic molecules exhibiting a large bending, inversion and internal rotation motion.

Finally, though the current version of the TENSOR code is dedicated to molecules exhibiting only 1 LAM, its extension to N_ρ large amplitude coordinates (*e.g.* the hydrazine or methylamine molecule[63]) could be carried out with only few modifications. As recalled by Bunker and Jensen[74] in their Eqs. (15-14) and (15-15), the new inertia matrix will be of dimension $(3+N_\rho)\times(3+N_\rho)$, with some coupling terms between the different LAM coordinates ρ_1, ρ_2, etc. Thus, the HBJ Hamiltonian could be expressed in terms of $3N-6-N_\rho$ normal-mode coordinates and of the $3+N_\rho$ rotational components J_x, J_y, J_z, J_{ρ_1}, J_{ρ_2}, etc.

C. Tensorial Hamiltonian and dipole moment operators on a numerical grid: the hybrid model

1. Symmetry considerations

We just recall here the basic principles and main definitions that can be useful when dealing with symmetry which plays a central role in nonrigid molecules. Indeed, the formidable development in experimental techniques make it possible to resolve small tunnelling splittings that are calculated quantum-mechanically while group theory provides meaningful labels. It is not the purpose of the present work to give a detailed review of all the symmetry properties of a given molecule and to study how the vibration-LAM-rotation wave functions transform in the operations of a symmetry group. Extensive group-theoretical considerations can be found for example in the excellent reviews[66,67,69,73,74,106–108] (and references therein).

By definition, a CNPI group is the direct product of permutation groups $\mathcal{S}_m$ with the inversion group $\varepsilon = \{E, E^*\}$ where E^* is the laboratory-fixed inversion operation. For example, the CNPI group G_n consists of n nuclear permutation and nuclear permutation inversion operations. A molecular symmetry group is formed by all "feasible" operations of the CNPI group and can be denoted to as $G_{n'}$ ($n' \leq n$) or as $\mathcal{G}(M)$, where $\mathcal{G}$ is the corresponding point group. Typically, in the first version of the TENSOR computer code designed for semirigid molecules, both the Abelian (C_2, C_i, C_s, C_{2v},C_{2h}, D_2 and D_{2h}) and non-Abelian (D_n, C_{nv}, D_{nh} ($n \geq 3$), D_{nd}, T_d, O_h) point groups were implemented.

Non-tunnelling molecules: for molecules where no tunnelling splitting is observed, the extension of TENSOR to the MS groups is direct because of their isomorphism with the point groups. However, the MS group is not necessarily the same as the CNPI group. For example, for ammonia the CNPI group $\mathcal{S}_3 \times \varepsilon$ or G_{12} is isomorphic to the group $D_{3h}(M)$ or to the point group D_{3h} of the planar configuration while for phosphine G_{12} is not isomorphic to the group $C_{3v}(M)$ or C_{3v}.

Tunnelling molecules: if at least one barrier in the description of the LAM is not "insuperable", a tunnelling splitting may be observed and the analysis of spectra of nonrigid molecules will require the use of MS groups that can be significantly different from the point groups. It may also arise that the MS group of a tunnelling molecule is isomorphic to a point group, but most of the time it is not really possible to classify the states of molecules with a LAM using a familiar point group alone. For molecules containing identical coaxial rotors such as ethane or hydrogen peroxide, it is necessary to use an *extended* MS group[74] $G_m(EM) = G_m \times \{E, E'\}$, where the operation E' consists in increasing a rotational angle (χ_a or χ_b) by 2π. Such groups can be also isomorphic to a point group (*e.g.* $G_4(EM) \sim D_{2h}$ for hydrogen peroxide).

More generally, for symmetry groups consisting of many operations, we have to face with the determination of the character tables and symmetry species which can be tedious. In this context, Hougen[109] presented a series of "recipes" aiming at helping the user to handle permutation-inversion groups for practical spectroscopic applications. As stated by Woodman[67], the most common way to handle a large MS group is to find a structure with smaller subgroups. Indeed, many large groups can be expressed as a *group product*, making easier the determination of the symmetry species and generators. For example, for ethane-like molecules we have the direct product structure[72] $G_{36} = C_{3v}^+ \times C_{3v}^-$, consisting of 36=6×6

feasible operations, where $+/-$ is used to distinguish the two methyl groups. It was also shown in Ref.[67] that the symmetry groups of nonrigid molecules can be expressed as semi-direct products of the type $\mathcal{A} = \mathcal{B} \wedge \mathcal{C}$ if only $\mathcal{B}$ is an invariant subgroup of $\mathcal{A}$. Alternatively, a method based on the nonrigid group theory[69,110] was also proposed to handle very large MS groups.

Once the character table and generators of a given MS group known, the Clebsch-Gordon coupling coefficients as well as the recoupling 6C and 9C Wigner's symbols involved in the calculation of matrix elements (see Eq. (30) below) can be thus deduced. For example, the Clebsch-Gordon coefficients adapted to a MS group can be computed by following the method presented in Ref.[111]. A set of irreducible tensor operators for the small-amplitude vibrational, rotational and large-amplitude vibrational motions as well as symmetry-adapted vibration-LAM-rotation wavefunctions can be also deduced from symmetry considerations.

We will assume hereafter that the character table, multiplication table and symmetry species Γ_i of a given MS group are known in order to (i) compute and store the coupling, recoupling and other related coefficients involved in the tensorial formalism and (ii) find the transformation laws of the wavefunctions in the operations of the MS group. The general theory presented in Section II as well as in the subsections III C 2, III C 3 and III C 4 below is now implemented in the updated version of TENSOR.

2. Hybrid Hamiltonian

For asymmetric top molecules with only one-dimensional irreps, accounting for symmetry is trivial because matrix and character coincide in group theory. Conversely, dealing with non-Abelian groups whose the dimension of some irreps may be greater than 1 is somewhat more challenging and requires more attention. For example, two-fold or three-fold degenerate vibrations are involved for point groups characterized by the presence of a symmetry axis higher than two-fold or in MS (or double) groups like G_6, G_{12}, G_{24}, G_{36}, etc. Within this context, the use ITOs is relevant to deal with degenerate vibrational modes like ν_3 and ν_4 of the NH_3 molecule. Historically, and still nowadays, the ITOs were introduced to analyse vibration-rotation infrared spectra of methane-like T_d molecules using effective polyad models and the so-called tetrahedral formalism[112]. They have been extended later on to other molecular species in various formalisms[113–116]. More recently, we have shown that the ITOs

could be also used for the construction of complete nuclear-motion Hamiltonians and *ab initio* dipole moment operators[88]. They were thus employed with success in the construction of spectroscopic line lists of semirigid molecules from the first-principles[13,21,51–53].

In the present work, a HBJ-based nuclear-motion tensorial Hamiltonian for nonrigid molecules is considered for the very first time. For a given value ρ_m, the "initial" HBJ Hamiltonian $H^{HBJ}_{\rho_m} = T^{HBJ}_{\rho_m} + V_{\rho_m}$ writes as a sum of products and takes the simple form

$$H^{HBJ}_{\rho_m} = \sum_j h_j(\rho_m)\mathcal{T}_j, \tag{15}$$

where $\boldsymbol{\mathcal{T}}$ is a vector whose each entry contains a specific operator

$$\mathcal{T}_j = \left(\prod_{k=1}^{3N-7} Q_k^{m_{j,k}} P_k^{n_{j,k}} \right) J_\rho^{n_{j\rho}} J_\alpha^{n_{j\alpha}} J_\beta^{n_{j\beta}}. \tag{16}$$

By considering all the values ρ_m in (2), the Hamiltonian parameters can be stored in a 2-dimensional array, that is $h_j(\rho_m) \equiv h_{jm}$. Each row is a parameter associated with a given operator $\mathcal{T}_j$ and each column is a point of the numerical grid (2). At this stage, we follow the strategy previously established for semirigid molecules and assume that the Hamiltonian (15) can be rearranged into a sum of vibration-LAM-rotation ITOs

$$H^{HBJ}_{tens,\rho_m} = \sum_{j=1} \left({}^{\varepsilon}V_j^{\Omega_v(\Gamma_v)} \otimes \left(L_{j,\rho_m}^{\Omega_\rho(\Gamma_{\rho 1}\Gamma_{\rho 2},\Gamma_\rho)} \otimes R_j^{\Omega_r(K_r,\alpha_r\Gamma_r)} \right)^{(\Gamma_{\rho r})} \right)^{(\Gamma_{v\rho r})}. \tag{17}$$

Each operator involved in the sum must transform as the totally symmetric irrep Γ_0 of the MS group, *i.e.* $\Gamma_{v\rho r} = \Gamma_0$. In Eq. (17), V, R and L stand for the vibrational, rotational and LAM irreducible tensors of degree Ω_v, Ω_r and Ω_ρ in (Q,P), (J_x,J_y,J_z) and J_ρ, respectively. ε is the parity in the conjugate momenta P such that $\varepsilon = (-1)^{\Omega_r+\Omega_\rho}$ due to the time reversal invariance. More details about the definition and construction of V and R can be found elsewhere[112,115–121], even for open-shell molecules in a degenerate electronic state[122–126], but only in the frame of effective polyad Hamiltonians using creation-annihilation operators. Our vibrational ITOs can be built in various coordinate systems and account for all intra-polyad coupling terms.

Briefly, the vibrational part V is built as the tensor product of $N_m - 1$ operators $V_k^{\Theta_k(\Gamma_k)}$ where N_m is the total number of vibrational modes, while the single mode associated with the LAM is incorporated into L. Each $V_k^{\Theta_k(\Gamma_k)}$ is constructed from the symmetrized powers

$\mathcal{Q}_k$ and $\mathcal{P}_k$ of degree Ω_{kq} and Ω_{kp} in the small amplitude coordinates $Q_s^{(\Gamma)}$ and conjugate momenta and $P_s^{(\Gamma)}$ involved in the vibrational mode k

$$V_{k,\sigma_k}^{\Theta_k(\Gamma_k)} = \left(\mathcal{Q}_k^{\Omega_{qk}(\boldsymbol{\alpha_q}_k\Gamma_{qk})} \otimes \mathcal{P}_k^{\Omega_{pk}(\boldsymbol{\alpha_p}_k\Gamma_{pk})}\right)_{\sigma_k}^{(\Gamma_k)}, \tag{18}$$

where all the intermediate quantum numbers and symmetry labels are stored in $\boldsymbol{\alpha_q}$ and $\boldsymbol{\alpha_p}$. Here, $\Omega_v = \sum_k \Omega_{qk} + \Omega_{pk}$ and σ_k is a component when $dim(\Gamma_k) > 1$. The rotational part R is built recursively in terms of J_x, J_y and J_z, K_r is the rank of the tensor in SO(3) and α_r is a rotational labelling that will be different for spherical, symmetric and asymmetric-top molecules (see Section III C 4).

Finally, we define in this work the LAM operators as

$$L_{j,\rho_m}^{\Omega_\rho(\Gamma_{\rho 1}\Gamma_{\rho 2},\Gamma_\rho)} = s_j(\rho_m)\left(I^{(\Gamma_{\rho 1})} \otimes \mathcal{J}^{\Omega_\rho(\Gamma_{\rho 2})}\right)^{(\Gamma_\rho)}, \tag{19}$$

where $\mathcal{J}$ is an operator of degree Ω_ρ in J_ρ and of symmetry $\Gamma_{\rho 2}$. To be consistent, the ρ-dependent tensorial parameters s_j to be determined have been naturally included into L. The identity operator I introduced in (19) reflects the fact that the LAM function $s_j(\rho)$ possesses a certain symmetry $\Gamma_{\rho 1}$ in the MS group (see Fig. 2). Usually, there are 2 types of symmetry species $\Gamma_{\rho 1}$ for non-tunnelling molecules or for molecules with one tunnelling like ammonia for which $\Gamma_{\rho 1} = A_1'$ or A_2''. When dealing with several tunnellings, more symmetry species $\Gamma_{\rho 1}$ can be involved. For example, the allowed symmetry species $\Gamma_{\rho 1}$ of the extended MS group $G_4(EM)$ will be A_{gs}, A_{us}, A_{gd} and A_{ud} for the H_2O_2 molecule. Note that H_2O_2 is among these molecules for which the symmetry species of a point group (here, D_{2h}) can be used due to the one-to-one mapping of its elements with those of $G_4(EM)$.

The last step in the construction of the tensorial model is the determination of the parameters $s_j(\rho_m)$. To this end, we expand the vibrational, rotational and LAM ITOs in terms of elementary operators using the Clebsch-Gordan coefficients (*e.g.* see Eq. (21) of Ref.[98]), sorted in such a way that the Hamiltonian (17) writes as

$$H_{tens,\rho_m}^{HBJ} = \sum_j s_j(\rho_m) Z_{jk} \mathcal{T}_k, \tag{20}$$

where $\mathbf{Z}$ is a group symmetry transformation. By equating Eqs. (15) and (20) and bearing in mind that the two sums involved in these two equations do not necessary contain the same number of terms if degenerate vibrations are involved, a set of parameters $\{s_j\}$ is obtained

by solving for each point ρ_m the following overdetermined system of equations

$$\mathbf{Z}^t\mathbf{s}(\rho_m) = \mathbf{h}(\rho_m). \tag{21}$$

In order to solve this least squares problem, the *dgels* routine of the LAPACK library was used. It takes generally few seconds per point ρ_m to solve (21) and obtain a set of tensorial parameters $\{s_j\}$. As an illustrative example, let us consider four vibration-rotation-torsion coupling terms between the $\nu_4(A_{1u})$, $\nu_5(B_{1u})$ and $\nu_6(B_{1u})$ modes of H_2O_2 written in the form (17) as

$$\begin{aligned} H^{\text{coupling}}_{tens,\rho_m} = \; & s_1(\rho_m)((Q_6^{(B_{1u})} \otimes J_\rho^{(A_u)})^{(B_{1g})} \otimes R^{1(1,0B_{1g})})^{(A_g)} \\ & + s_2(\rho_m)((Q_5^{(B_{1u})} \otimes (Q_6^{(B_{1u})})^2 \otimes P_6^{(B_{1u})})^{(B_{1u})})^{(A_g)} \otimes R^{1(1,1B_{2g})})^{(B_{2g})} \\ & + s_3(\rho_m)((Q_6^{(B_{1u})})^3 \otimes R^{1(1,1B_{3g})})^{(B_{2u})} \\ & + s_4(\rho_m)((Q_6^{(B_{1u})})^3 \otimes R^{1(1,0B_{1g})})^{(A_u)} + \cdots \end{aligned} \tag{22}$$

where the symmetry species of D_{2h} are used here instead of those of $G_4(EM)$. The four parameters s_j are plotted in Fig. 2 for each value ρ_m from 0 to 4π. In order to check the overall symmetry of the Hamiltonian (22), these four grids composed of 100 points have been fitted by analytical functions. When dealing with internal rotation, it is quite obvious that the Fourier series ($\cos(k\rho/2)$, $\sin(k\rho/2)$) are well adapted to describe periodic functions, where the symmetry species will depend on the parity of k, also related to the parity K of a rotational wave function (K is the projection of J on the molecule axis z). In our case, we obtain

$$\begin{aligned} s_1(\rho) &= -1.031 + 0.274\,\cos(\rho) - 0.012\,\cos(2\rho) + 0.0022\,\cos(3\rho) + \cdots && \longrightarrow A_g, \\ s_2(\rho) &= -0.0012\,\sin(\rho/2) - 0.0011\,\sin(3\rho/2) + 0.0007\,\sin(5\rho/2) + \cdots && \longrightarrow B_{2g}, \\ s_3(\rho) &= -0.0009\,\cos(\rho/2) + 0.0008\,\cos(3\rho/2) - 0.0001\,\cos(5\rho/2) + \cdots && \longrightarrow B_{2u}, \\ s_4(\rho) &= 0.0001\,\sin(\rho) - 0.0005\,\sin(2\rho) + 0.0001\,\sin(3\rho) + \cdots && \longrightarrow A_u, \end{aligned} \tag{23}$$

and according to the operations $E^*(\rho/2) = \pi - \rho/2$ and $E'(\rho/2) = \pi + \rho/2$, the functions $s_1(\rho)$, $s_2(\rho)$, $s_3(\rho)$ and $s_4(\rho)$ transform as A_g, B_{2g}, B_{2u} and A_u, making the Hamiltonian (22) totally symmetric. We can thus see that the A_g/A_u functions are 2π-periodic while the B_{2g}/B_{2u} functions are 4π-periodic. Note that only the A_g/A_u species are involved in the vibration-LAM Hamiltonian.

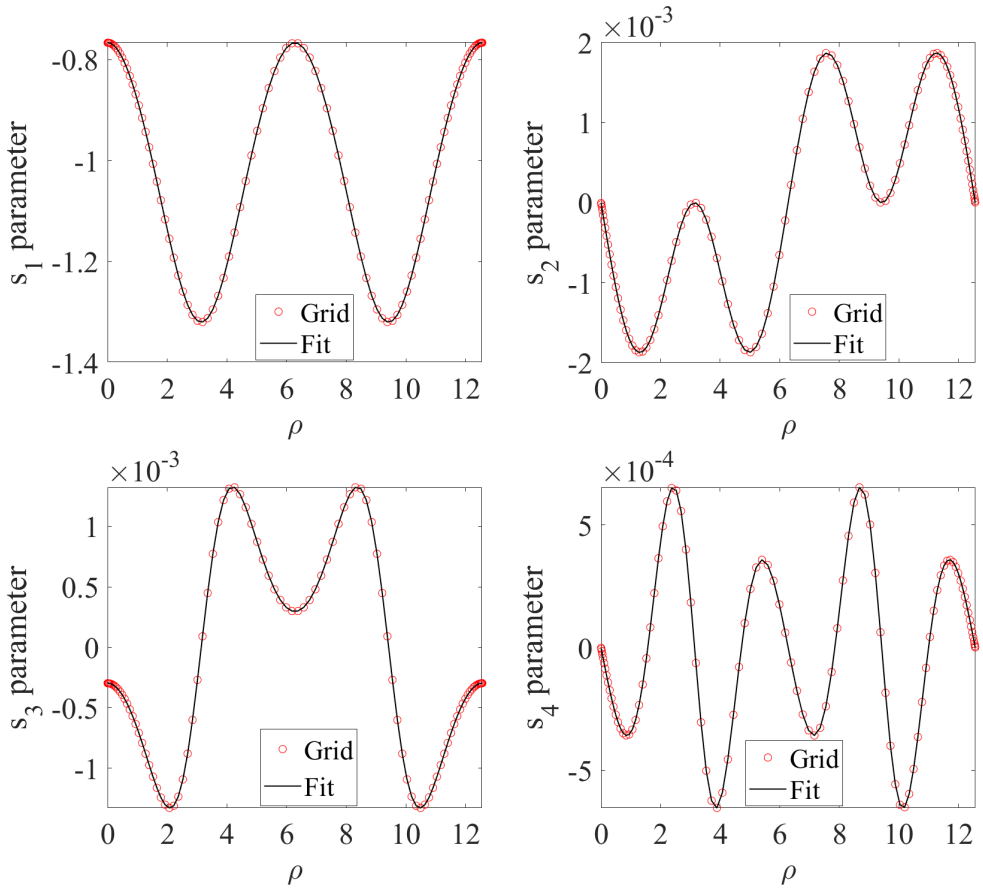

FIG. 2. Plot of the four parameters s_j $(j = 1, \cdots, 4)$ of the Hamiltonian (22) for each point ρ_m (red circles) for H_2O_2 (see also Section IV). Each grid has been fitted using Fourier series (see Eq. (23)) transforming respectively as the A_g, B_{2g}, B_{2u} and A_u irreps of D_{2h} (solid line).

3. Hybrid dipole moment

For the line intensity calculation of vibration-LAM-rotation transitions, we first have to relate the components $({}^S\mu_X, {}^S\mu_Y, {}^S\mu_Z)$ of the space-fixed dipole moment to the molecule-fixed frame components $({}^m\mu_x, {}^m\mu_y, {}^m\mu_z)$ *via* the direction cosines. We assume here the isotropy of the three dimensional space, so only the Z component is required. In order to be consistent with the hybrid Hamiltonian model, (i) the Eckart-Sayvetz conditions are used for the orientation of the molecule-fixed frame (xyz) to conveniently define the *ab initio* components ${}^m\mu_\alpha$ and (ii) symmetry-adapted ITOs are used for the construction of

the space-fixed frame Z component as follows:

$$ {}^{S}\mu^{(\tilde{\Gamma})}_{Z,\rho_m} = \left({}^{m}\mu^{(\Gamma_{v\rho})}_{tens,\rho_m} \otimes \mathcal{C}^{(\Gamma)} \right)^{(\tilde{\Gamma})}. \tag{24} $$

The ITOs ${}^{m}\mu^{(\Gamma_{v\rho})}_{tens,\rho_m}$ have a form similar to (17) but with different symmetry species and are constructed on the same grid as H. Moreover, we have the condition $\Omega_p = \Omega_\rho = \Omega_r = 0$. The tensor dipole moment parameters are determined by solving a system of equations like (21) for each ρ_m. In Eq. (24), $\mathcal{C}$ is the direction cosine tensor[112].

Finally, the quality of the line intensity calculation will be governed by two ingredients: the calculation of the eigenpair $\{E, \Psi\}$ by solving the time-independent Schrödinger equation and an accurate dipole moment surface whose the construction is beyond the scope of this work.

4. Hamiltonian matrix elements and choice of the LAM grid

In order to compute the matrix elements of the Hamiltonian (17), we have to pay attention to the choice of the numerical grid (2) to simplify calculations. To this end, let us first consider the LAM Hamiltonian obtained by setting $V = R = I$ in (17)

$$ H^{LAM}_{\rho_m} = s_1(\rho_m) + s_2(\rho_m) J_\rho + s_3(\rho_m) J^2_\rho. \tag{25} $$

This Hamiltonian can be also seen as the analytical Hamiltonian

$$ H^{LAM}(\rho) = s_1(\rho) + s_2(\rho) J_\rho + s_3(\rho) J^2_\rho, \tag{26} $$

evaluated at $\rho = \rho_m$, where the $s_j(\rho)$ are not necessary known functions, though some of them could be easily related to the potential or to the tensor inertia matrix. For example, $s_1(\rho)$ writes as $a\rho^4 - b\rho^2 + \cdots$ for an inversion potential or $s_1(\rho)$ is expressed as a Fourier series for a torsional potential, while $s_3(\rho) \sim \mu^{\mathrm{ref}}_{\rho\rho}(\rho)/2$. If we consider a set of LAM basis functions $\phi^{(C_\rho)}_{v_\rho}$ of symmetry C_ρ, the matrix elements for each term of the Hamiltonian (26) can be computed numerically using the standard quadrature formula

$$ \mathcal{L}^j_{v'_\rho v_\rho} = \sum_m \phi^{(C_\rho)}_{v'_\rho}(\rho_m) s_j(\rho_m) J^{n_j}_\rho \phi^{(C_\rho)}_{v_\rho}(\rho_m) w_m. \tag{27} $$

where v_ρ is the principal LAM quantum number taking values 0, 1, $\cdots$ and w_m are the quadrature weights. It is thus demonstrated after a brief inspection of Eqs. (25) and (27)

that the computation of the matrix elements for the LAM problem is greatly simplified if a set of M_ρ quadrature points is used to define the grid (2). In that case, we just need to read the stored parameters $s_j(\rho_m)$ of the LAM Hamiltonian (15) to compute the matrix elements (27). In this work, a Gauss-Legendre quadrature of $\sim$100 points at the quadruple precision was considered to make a numerical integration between ρ_{min} and ρ_{max}. Moreover, the quadrature points generally go around singularity points *e.g.* the singularity in $\mu_{\alpha\beta}$ at the linear configuration of a triatomic molecule is avoided because the first quadrature point takes a nonzero positive value when integrating from $\rho_{min} = 0$ to ρ_{max}.

Let us now focus on the calculation of the matrix elements for the parts V and R. In order to compute the matrix elements of the full Hamiltonian (17), Eq. (26) can be generalized to the whole vibration-LAM-rotation problem and the superscript j in Eq. (27) will run over all the vibration-LAM-rotation tensor operators. The key of the present approach is thus to compute and store in memory the matrix elements $\mathcal{L}^j_{v'_l v_l}$ in a LAM basis set of all the ρ-dependent Hamiltonian parameters. This procedure takes few seconds because the LAM basis contains generally less than 20 functions and the Hamiltonian has few hundreds or thousands parameters.

In order to be consistent with the Hamiltonian coupling scheme, our vibration-LAM-rotation basis functions are written as

$$\Phi^{(C_{v\rho r})}_{\sigma_{v\rho r}} = \left(\Phi^{(C_v)}_{v} \otimes \left(\Phi^{(C_\rho)}_{v_\rho} \otimes \Phi^{(J,\alpha C_r)}_{rot} \right)^{(C_{\rho r})} \right)^{(C_{v\rho r})}_{\sigma_{v\rho r}}, \tag{28}$$

where Φ_v, Φ_{rot} and Φ_{v_ρ} are symmetry-adapted vibrational, rotational and LAM functions, respectively, described briefly as follows.

Small amplitude basis functions: The vibrational function Φ_v is a product of $N_m - 1$ harmonic oscillator functions. Their construction is trivial for non-degenerate modes. The treatment of two- and three-fold degenerate vibrations require more attention. For example, a method was proposed in Ref.[115] in the case of C_{3v} and T_d molecules and extended later on to arbitrary point groups[127]. The treatment of MS groups can be carried out in the same fashion.

Rotational basis functions: The construction of the symmetry-adapted Φ_{rot} rotational functions will depend on which family the molecule belongs. For spherical top molecules, a method was proposed in Ref.[128] to build such functions for both integer and half-integer J values, that is for both vectorial ans spinorial representations[129]. In that case, α in (28)

plays the role of a multiplicity index. For symmetric and asymmetric tops, we can consider symmetrized Wang-type basis functions

$$\Phi_{rot,\sigma_r}^{(J,kC_r)} = \sum_{K=\pm k} {}^{(J)}G_{\Gamma_r\sigma_r}^{K}\Phi_K^{(J)}. \tag{29}$$

where the G coefficients, including a consistent choice for the phase factors, have been also determined[127] for arbitrary point groups and implemented in TENSOR. Again, its extension to MS groups can be carried out quite easily.

Large amplitude basis functions: The choice of the functions Φ_ρ will depend on the nature of the LAM (Section IV).

In the present study, the matrix elements are computed from a symmetry adaptation of the standard Wigner-Eckart theorem in SO(3) found in many textbooks of quantum mechanics and group theory[130] for the small amplitude vibration and the rotation parts, combined with a numerical integration for the LAM part. The matrix elements for each term of the sum in Eq. (17) are given by

$$\begin{aligned}
&\left\langle \Phi_{\sigma'_{v\rho r}}^{(C'_{v\rho r})} \mid (VLR)_j \mid \Phi_{\sigma_{v\rho r}}^{(C_{v\rho r})} \right\rangle = [C_{v\rho r}]([\Gamma_{\rho r}^j][C_{\rho r}][C'_{\rho r}])^{1/2} \begin{Bmatrix} \Gamma_v^j & C_v & C'_v \\ \Gamma_{\rho r}^j & C_{\rho r} & C'_{\rho r} \\ \Gamma_0 & C_{v\rho r} & C_{v\rho r} \end{Bmatrix} \\
&\times \begin{Bmatrix} \Gamma_\rho^j & C_\rho & C'_\rho \\ \Gamma_r^j & C_r & C'_r \\ \Gamma_{\rho r}^j & C_{\rho r} & C'_{\rho r} \end{Bmatrix} \left(\phi^{(J,\alpha' C'_r)} \mid\mid R_j^{\Omega_r(K_r,\alpha_r\Gamma_r)} \mid\mid \phi^{(J,\alpha C_r)} \right) \delta_{\sigma'_{v\rho r}\sigma_{v\rho r}} \delta_{C'_{v\rho r}C_{v\rho r}} \\
&\times \mathcal{M}_v^j \prod_{k=1}^{N_m-1} \left(\Phi_{v'_k}^{(C'_{vk})} \mid\mid V_{k,j}^{\Theta_k(\Gamma_k)} \mid\mid \Phi_{v'_k}^{(C'_{vk})} \right) \longrightarrow \text{Rigid vibrations} \\
&\times \mathcal{L}_{v'_\rho v_\rho}^j \qquad\qquad\qquad\qquad\qquad\qquad \longrightarrow \text{Nonrigid vibration(s)}
\end{aligned} \tag{30}$$

In this expression, $(\cdots \mid\mid V \mid\mid \cdots)$ and $(\cdots \mid\mid R \mid\mid \cdots)$ are vibrational and rotational reduced matrix elements[112,115] and the $9C$ are the recoupling Wigner's symbols computed from the symmetry-adapted Clebsch-Gordan coefficients (see *e.g.* Ref.[111] for their definition). The rotational reduced matrix elements involved the so-called isoscalar factors which are computed from the G coefficients in (29), the Clebsch-Gordon coefficients as well as the $3j$ Wigner symbols. $[C]$ is the dimension of the irrep C and $\mathcal{M}_v^j$ is a factor that contains a product of $9C$ symbols characterizing the vibrational inner coupling scheme. $\mathcal{L}_{v'_\rho v_\rho}^j$ are the matrix elements (27) of the LAM operators computed by numerical quadrature. From

the selection rules, the use of symmetry thus allows to diagonalize separately each block labelled by J and $C_{v\rho r}$. The computation of the matrix elements for the dipole moment will be similar.

Finally, our hybrid model combines the rapidity of group-theoretical methods (*via* the use of ITOs and of the Wigner-Eckart theorem) for the rigid part and the flexibility of the numerical quadrature integration for the nonrigid part. All the elements (30) are generally computed from few seconds up to some tens of minutes by using standard libraries for a massive parallel programming, even for large basis sets composed of $\sim$ 100000 functions. Here, all the matrices were diagonalized using direct eigensolvers.

5. Reduced Hamiltonian and reduced vibrational eigenvectors

One of the main advantages of using the Watson or HBJ Hamiltonian lies in the fact that the form of their KEO remains unchanged, whatever the number of atoms. In turn, the number of terms in the Hamiltonian (15) may increase dramatically when performing a Taylor series expansion of the multivariate $\mu_{\alpha\beta}$ and V functions. A similar problem arises when managing the number of vibration-LAM functions in the direct-product basis (28) to compute variational solutions for $J > 0$. The number of rovibrational functions becomes rapidly huge, even by pruning the basis using Eq. (32).

In order to make vibration-LAM-rotation calculations as tractable as possible for the user, a strategy was proposed in Refs.[13,88–90] for semirigid molecules in order to drastically reduce the number of terms in the sum (15) as well as the number of basis functions, with a small loss of precision. We propose here to apply the same strategy for nonrigid molecules, with illustrative examples given in Section IV. Very briefly:

Reduced Hamiltonian: the p-order polynomial expansion (15) expressed in terms of $(Q_i, P_i, J_\rho, J_\alpha)$ is first transformed into a second-quantized form in terms of $(a_i^+, a_i, J_\rho, J_\alpha)$. Then, we define a new order $p' < p$ and we discard during the second-quantized transformation all the terms of degree $> p'$ in a^+ and a. In a final step, a backward transformation of the low-order second-quantized Hamiltonian allows to define a so-called reduced Hamiltonian

$$H_{\rho_m}^{HBJ} \longrightarrow H_{red,\rho_m}^{HBJ}. \tag{31}$$

Then, the "pure" Taylor-based expansion (15) is substituted by (31). This procedure can be thus seen as a polynomial reduction where an initial p-order polynomial is transformed

to a p'-order polynomial. The advantage of this method is twofold: it allows reducing the number of terms by at least one order of magnitude and it generally allows getting rid of artefacts and spurious minima inherent to the high-order Taylor expansion of multivariate functions.

Reduced eigenvectors: the $J = 0$ problem is first solved by using a suitable vibrational basis $F(m)$ (see Eq. (32)) to converge properly the desired eigenvalues. Then, we select relevant vibrational eigenvectors, we define so-called reduced eigenvectors $\Psi_{red}^{(m\rightarrow m')}$, or simply denoted to as the $F(m \rightarrow m')$ reduction with $m' < m$, and we compute the rovibrational solutions by following the procedure described by Eqs. (7)−(11) of Ref.[90].

IV. APPLICATIONS

In order to validate our HBJ-based hybrid model, we consider in this section four molecules with one "floppy' large amplitude vibration: the quasilinear CH_2 methylene molecule, the planar CH_3 methyl radical, the NH_3 ammonia molecule with inversion and the H_2O_2 hydrogen peroxyde molecule with internal rotation. It is worth mentioning that the proposed hybrid model was recently used to validate our new PESs[131–133], but described in a very sparse manner. In this work, the theory as well as the methodology illustrated with practical applications are presented with more details.

Beyond the necessary validation step, this section also aims at carefully studying the impact of the Hamiltonian and basis set truncation on the energy level calculation. Recent papers[89,134] studied the dependence of rovibrational calculations with respect to the truncation order of the Watson Hamiltonian. A similar convergence study is proposed here for nonrigid molecules and turns out very relevant for

(i) controlling carefully the precision of the calculated eigenvalues and eigenvectors,

(ii) constructing a tailor-made model suitable either for the analysis of high-resolution spectra or for the modelling of some planetary atmospheres requiring less accuracy.

As usual, we discard in our variational calculation all the rigid and LAM vibrational basis functions that do not satisfy the pruning condition

$$F_\kappa(p) = \kappa_\rho v_\rho + \sum_{i=1}^{3N-7} \kappa_i v_i \leq p, \quad v_\rho, v_i = 0, \cdots, p, \tag{32}$$

where κ_ρ, κ_i are some weight coefficients. Combined with symmetry, this condition can

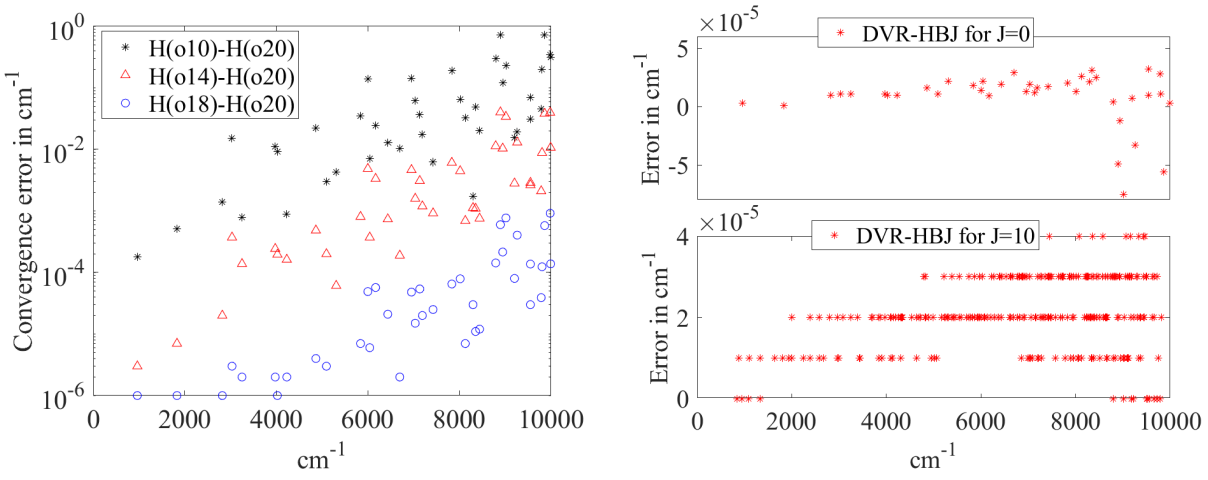

FIG. 3. (Left panel) Convergence of the $J = 0$ energies for CH_2 using the $F(27)$ basis set as a function of the Hamiltonian order (17) with respect to the energies obtained from the model truncated at order 20. (Right panel) Error between DVR[135] and variational/HBJ (this work, using the $F(27)$ basis set and the hybrid Hamiltonian truncated at order 20) calculation for $J = 0$ and $J = 10$.

reduce drastically the dimension of the Hamiltonian matrix to be diagonalized by several orders of magnitude. Note that in all the calculations below, the rigid part of the Hamiltonian (17) was rewritten in terms of dimensionless normal coordinates and conjugate momenta (q, p) using the standard relation $q = \gamma^{1/2}Q$.

A. CH_2 molecule

These past four decades, published papers were dedicated to the energy level calculation and line transition prediction of methylene in its ground electronic triplet state[136–140]. Due to its large bending motion with a low barrier to linearity around 2000 cm^{-1}, methylene turns out a good first candidate to validate our hybrid model. A recent accurate *ab initio* PES for CH_2 has been calculated[133], including both relativistic and diagonal Born-Oppenheimer corrections as well as high-order electronic correlations. This PES will be naturally used in the present paper for various validation tests.

Our grid is composed of 100 quadrature Gauss-Legendre points and the hybrid Hamiltonian (17) was computed from $\rho_{min} = 0$ to $\rho_{max} = 3.1$ radians. The construction of the symmetrized powers for the two stretching coordinates is trivial when dealing with one-

dimensional irreps. Indeed, for a symmetry species Γ, the symmetrized powers will be just Γ_0 (resp. Γ) for even (resp. odd) powers. The standard harmonic oscillator basis functions (HOBF) were used for the stretching modes while the displaced HOBF $N_v H_v(\rho')e^{-\rho'^2/2}$, with $\rho' = 5(\rho - 0.7)$, multiplied by a weight function $\sqrt{\sin(\rho)}$ were chosen for the bending mode to properly treat the overall range of ρ, even near $\rho = 0$. These functions are ortho-normalized using the standard Gram-Schmidt technique.

As a first test, the convergence of the KEO and potential developed in terms of q_1 and q_3 was studied. To this end, we have compared in Fig. 3 (left panel) the $J = 0$ energy levels obtained from the Hamiltonian (17) truncated at order 10, 14, 18 with respect to those obtained from the Hamiltonian truncated at order 20, taken as the benchmark calculation. The 10^{th}, 14^{th}, 18^{th} and 20^{th} order Hamiltonians contains 378, 778, 1332 and 1648 ITOs, respectively. The $F(27)$ basis set defined in (32) and composed of 2135 A_1 functions and 1925 B_2 functions was used to compute the vibrational energy levels, which are converged within 10^{-4} cm^{-1} up to 10000 cm^{-1} using the Hamiltonian truncated at order 18. In Fig. 3 (right panel), we show that our $J = 0$ and $J = 10$ levels are in very good agreement with those obtained from the DVR3D computer code[135]. Indeed, using the 20^{th} order Hamiltonian and the $F(27)$ basis, the error on the $J = 0$ and $J = 10$ levels between DVR and our variational calculation is of 10^{-5} cm^{-1} up to 10000 cm^{-1}. For $J = 10$, the basis contains about 22000 functions but can be drastically reduced by choosing conveniently the weights κ_i in (32). For example, if $\kappa_1 = \kappa_3 = 1.2$ the number of basis functions is decreased by 35% and the rms error becomes 0.0002 cm^{-1} up to 10000 cm^{-1}. By taking 50% less functions ($\kappa_1 = \kappa_3 = 1.4$), the convergence of the levels is not fully achieved (rms error of 0.001 cm^{-1}) but the results remain suitable for high-resolution spectroscopy.

B. CH_3 molecule

The second candidate is the planar ($D_{3h}(M)$) methyl radical CH_3 for which the out-of-plane ν_2 mode exhibits a LAM behaviour. Recently, new *ab initio* CH_3 PES and DMS in its ground electronic state have been published[132] and are thus considered in this work. The hybrid Hamiltonian and dipole moment operator have been computed here on a numerical grid from $\rho_{min} = 0.41$ to $\rho_{max} = 2.69$ radians. The construction of the vibrational operators for the doubly degenerate modes ν_3 and ν_4 of symmetry E' in $D_{3h}(M)$ follows closely the

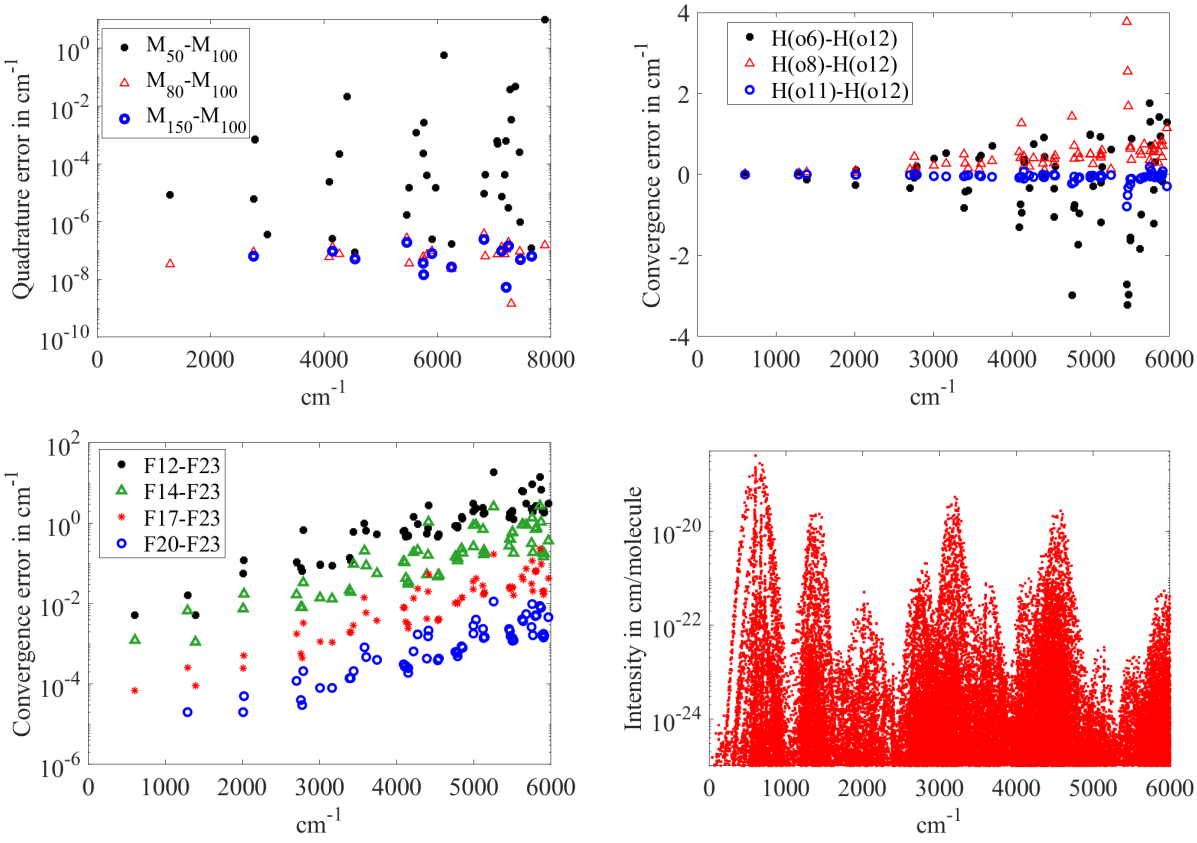

FIG. 4. Convergence error of the $J = 0$ energies for CH_3 as a function of the number of quadrature points (top, left panel), the Hamiltonian truncation order (top, right panel) and the basis set truncation (bottom, left panel), see text for more details. (Bottom, right panel) line intensities computed from the DMS presented inf Ref.[132]

method presented in Ref.[115] for the C_{3v} and T_d point groups. For twofold degenerate oscillators, it is common to introduce the auxiliary boson operators[141] b_1 and b_2 and form the products $b_1^l b_2^m \equiv (lm)$, like in the $u(2)$ formalism[121]. The same holds for the construction of the creation part with b_1^+ and b_2^+. It is quite straightforward to see how these operators transform using the generators of $D_{3h}(M)$ and to show that the two quantities

$$\begin{aligned} T_{\sigma_1}^{(lm,\Gamma_1)} &= (lm) + (ml) \\ T_{\sigma_2}^{(lm,\Gamma_2)} &= e^{i\phi(l,m)}(-i)[(lm) - (ml)] \end{aligned} \tag{33}$$

can be used to define our vibrational ITOs. Note that the phase conventions applied in this work are different from those in Ref.[115]. By introducing $j = l - m$, we have $\Gamma_1 = A_1'$ when $l = m$, $\Gamma_1 = A_1'$, $\Gamma_2 = A_2'$ for $j = 3p$ $(p \neq 0)$ and $(\Gamma_1, \sigma_1) = (E', a)$, $(\Gamma_2, \sigma_2) = (E', b)$

for $j = 3p + 1$ or $3p + 2$, with p an integer number. All the factor $e^{i\phi(l,m)}$ equal 1, except for $j = 3p + 2$ where it equals -1. For a mode of symmetry E'', the symmetry rules will slightly change. In the ITO formalism, the vibrational reduced matrix elements involved in (30) take a quite simple form when using the creation-annihilation operators involved in effective Hamiltonians. For this work, we have shown[127] that the reduced matrix elements of symmetrized powers for doubly degenerate modes can be also put in a closed form using the (q, p) formalism. Concerning the rotational part, the symmetries Γ_r, involved in (29) will differ according to the values of k, that is we will have $\Gamma_r = A'_1 + A'_2$ for $k = 6p$ ($p \neq 0$), $\Gamma_r = A''_1 + A''_2$ for $k = 6p + 3$, $\Gamma_r = E'$ for $k = 6p + 2$ or $k = 6p + 4$ and $\Gamma_r = E''$ for $k = 6p + 1$ or $k = 6p + 5$. Concerning the bending mode ν_2, simple HOBF $N_v H_v(\rho')e^{-\rho'^2/2}$, with $\rho' = 8.1\rho$, of symmetry A'_1 for v even and A''_2 for v odd, were used.

As a first test, the number of quadrature points M_ρ was gradually increased from 50 to 150 in order to see the impact on the energy level calculation. A variational calculation was performed for different M_ρ using the $F(23)$ basis with $\kappa_1 = \kappa_2 = 1.4$ and $\kappa_3 = 1.3$, resulting in 11010, 9857, 20849, 7869, 8861 and 16719 basis functions of symmetry A'_1, A'_2, E', A''_1, A''_2 and E'', respectively. The errors between the $J = 0$ levels computed from $M_\rho = 50$, 80 and 150 and those computed from $M_\rho = 100$, taken as the benchmark, are depicted in Fig. 4 (top left panel). We clearly see that $M_\rho = 50$ is not accurate enough for practical applications, while the results become very similar from $M_\rho = 80$.

In a second step, we have studied the convergence of the Hamiltonian expansion. Like for CH_2, we have gradually increased the order of the expansion (17) and computed the vibrational levels for a given basis set (here, $F(23)$). The errors between the energy levels computed from the Hamiltonian truncated at order 6, 8 and 11 and those computed from the Hamiltonian truncated at order 12 are given in Fig. 4 (top right panel). We can see quite large fluctuations beyond 5000 cm^{-1} between the order 12 and 11, proving that this latter was not yet properly converged to study highly-excited (ro)vibrational state.

In a third step, the convergence of the variational calculation has been studied using different basis sets, namely $F(12)$, $F(14)$, $F(17)$, $F(20)$ and $F(23)$. The number of vibrational basis functions of symmetry E' increases as 525, 1071, 2556, 5536 and 11010, respectively. It is seen in Fig. 4 (bottom left panel) that the convergence error of the vibrational levels up to 5000 cm^{-1} is about of 10^{-3} cm^{-1} using the $F(20)$ basis. The use of the $F(23)$ basis allows converging the levels within 10^{-4} cm^{-1} up to 5000 cm^{-1} and within 10^{-3} cm^{-1} up to

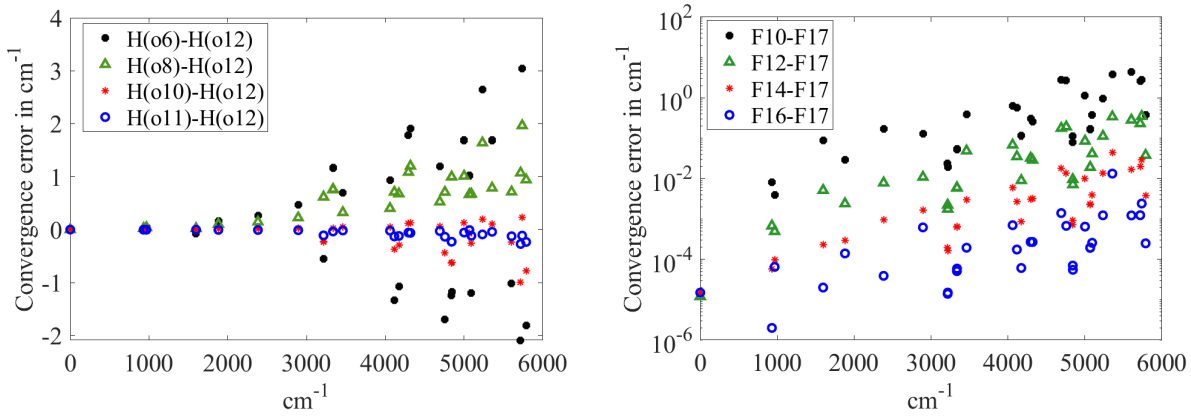

FIG. 5. Convergence error of the $J = 0$ energies for NH_3 as a function of the Hamiltonian truncation order (left panel) and the basis set truncation (right panel). See text for more details.

6000 cm^{-1}, which turns out enough for the modelling of high-resolution spectra. Finally, a room-temperature CH_3 line list up to 6000 cm^{-1}, including both cold and hot bands (see Fig. 4, bottom right panel) was constructed using the DMS presented in Ref.[132]. Comparisons with the results obtained in Ref.[142] can be also found in Ref.[132].

C. NH_3 molecule

The ammonia molecule is a good candidate to be tested using the hybrid model because its umbrella inversion is among the most prototypical cases of large amplitude motion. These past two decades, many works were devoted to the construction of refined PESs and published in the ExoMol group for the construction of molecular line lists[143] combined with a MARVELization procedure[144]. In this work, we have considered our recently published "pure" (*i.e.* in the sense without applying empirical corrections) *ab initio* PES[131] which turns out accurate up to 6600 cm^{-1}, with a root-mean-square error of 0.4 cm^{-1} between the calculated and observed levels (see Tab. 3 of Ref.[131]).

For this molecule, a grid $\rho \in [0.37, 2.83]$ radians was chosen to ensure a consistent energy calculation up to at least 6000 cm^{-1}. The construction of ITOs adapted to both the small amplitude vibrations and rotation is similar to the CH_3 molecule. The major difference lies in the treatment of the LAM, in particular in the choice of the basis functions adapted to the symmetric double-well potential. As usual, the two wells correspond to the two equivalent pyramidal $C_{3v}(M)$ equilibrium configurations. However, $C_{3v}(M)$ is no longer

suitable to describe the tunnelling because no operation in this group allows switching from one configuration to another one. Thus, for a proper classification of the overall vibration-inversion-rotation energy levels, we need to consider the larger permutation-inversion group G_{12} isomorphic to the MS group $D_{3h}(M) = C_{3v}(M) \times \{E, E^*\}$ and consisting of 8 feasible operations. In the case of ammonia, the tunnelling produces a splitting of the rigid-molecule $C_{3v}(M)$ states in two components which are deduced from the reverse correlation (or induction) table between $D_{3h}(M)$ and $C_{3v}(M)$. For example, the A_1 states split into A_1' and A_2'' components, the A_2 states split into A_1'' and A_2' components whereas the E states split into E' and E'' components. The question of how the energy levels of the infinite and low barrier limits are correlated was first raised by Watson[68].

Accordingly, a symmetric (A_1') and anti-symmetric (A_2'') linear combination of two displaced HOBF centered around the two potential wells can be used in the variational calculation as primitive basis functions for the inversion mode ν_2. In order to make the analogy with the field of quantum optics, the basis functions used here are nothing but a linear combination of displaced squeezed states (see *e.g.* Ref.[145] and references within) of the type

$$\Phi_{v,inv}^{(C)}(\rho) = \frac{1}{\sqrt{2}} \sum_{j=1}^{2} D(\lambda_j) S(k_j) e^{i\varphi_j(C)} \phi_v(\rho), \tag{34}$$

with $e^{i\varphi_1(C)} = 1$, $e^{i\varphi_2(A_1')} = 1$ and $e^{i\varphi_2(A_2'')} = -1$. The coherence ($\lambda_j$) and squeezing ($\kappa_j$) parameters play the role of variational parameters to be optimized. Here, the functions $\phi_v(\rho)$ are simply HOBF but Morse-like or Pöschl-Teller-like functions could be also used instead. The matrix elements $D_{vv'}$ and $S_{vv'}$ of the displaced and squeeze operators can be computed analytically[146].

Like for CH_2 and CH_3, the convergence of the Hamiltonian model is first studied and shown in Fig. 5 (left panel). To this end, we have computed the energy levels for the A_1' and A_2'' blocks composed of 17739 functions by using the $F(17)$ basis and by gradually increasing the Hamiltonian truncation order from 6 to 12. For the inversion motion, the new coordinate $\rho' = \rho - \pi/2$ was introduced for convenience so that the planar configuration is now defined at $\rho' = 0$. In this new coordinate system, the parameters of the basis function (34) have been defined as follows: $\kappa_1 = \kappa_2 = 9.45$ and $\lambda_1 = -\lambda_2 = 0.338$. We can thus estimate the precision of the Hamiltonian truncated at order 12 below 0.01 cm^{-1} up to 6000 cm^{-1}. Starting from this Hamiltonian model, we have then examined the convergence of the variational calculation by gradually increasing the number of basis functions. The results

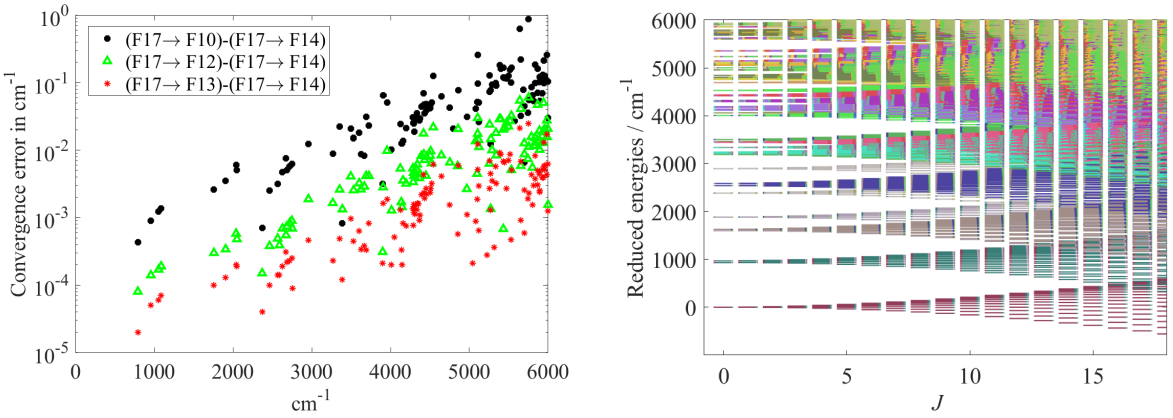

FIG. 6. (Left panel) Convergence error of the $J = 10$ energies for NH_3 as a function of the number of basis functions in the reduced basis (see text for more details). (Right panel) Reduced energy levels NH_3 up to J_{max}=18. The colours correspond to the mixing between the vibrational states.

are displayed in Fig. 5 (right panel). We can see that the energy levels using the $F(16)$ basis, which is composed of 13185, 11700 and 24864 A_1'/A_2'', A_1''/A_2' and E'/E'' functions respectively, are converged within 0.001 cm^{-1}, with the only exception for the level near 5356.1 cm^{-1} corresponding to $5\nu_2(A_2'')$. In that case, the use of the $F(17)$ basis composed of 17739, 15924 and 33642 A_1'/A_2'', A_1''/A_2' and E'/E'' functions is required to converge properly the 5-quanta vibrational bands. Needless to say that converging levels above 6000 cm^{-1} within 10^{-3} cm^{-1} will probably require more basis functions, in particular for the inversion mode.

For $J > 0$ calculations, the *reduced basis functions* $F(17) \rightarrow F(p)$ initially introduced for the rovibrational energy level calculation of semirigid molecules (see Section III C 5) have been tested for the NH_3 molecule for $J = 10$. The four weights κ_i associated with the $F(p)$ basis used here are 1.4, 1, 1.4, 1.3. In order to achieve a good convergence of the energy levels for the block $(J = 10, A_1')$, different values of p have been considered, namely $p = 10$, 12, 13 and 14. The dimension of the corresponding blocks are 7278, 16474, 23555 and 34111, respectively, while that without using reduced functions is of 354222. Thus, such functions allows to reduce the dimension of the problem by at least one order of magnitude and thus to use direct eigensolvers for the diagonalization. As usual, the biggest calculation corresponding to $p = 14$ will be taken as the benchmark.

The convergence of the levels with respect to p is depicted in Fig. 6 (left panel). We

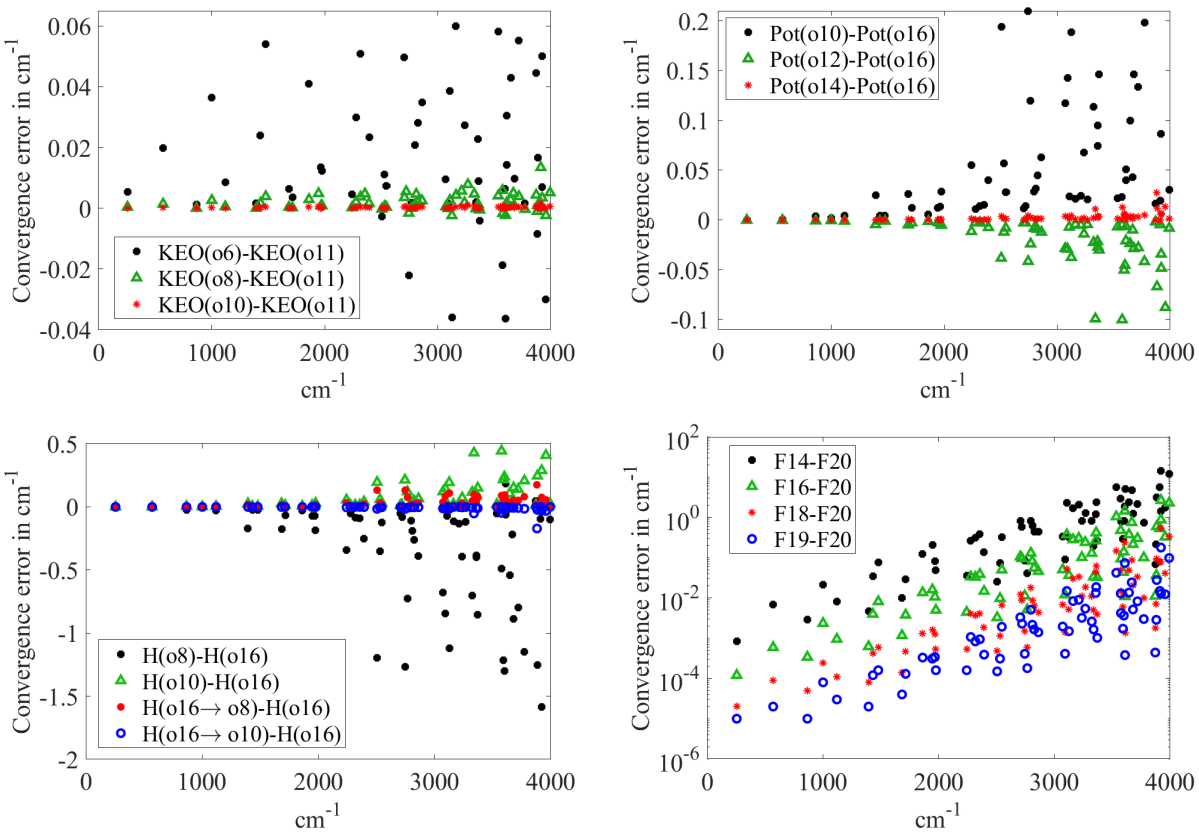

FIG. 7. Convergence error of the $J = 0$ energies for H_2O_2 with respect to the truncation order of (top, left panel) the kinetic energy operator (8), (top, right panel) the potential (7), (bottom, left panel) the reduced Hamiltonian (31) and (bottom, right panel) the basis set (32).

can see that the average error between $p = 13$ and $p = 14$ is 0.001 cm^{-1} up to 6000 cm^{-1}, which is the typical resolution of Fourier transform infrared spectra. Even the smaller basis ($p = 10$) can produce qualitatively correct results, with errors around 0.01 cm^{-1} or less up to 4000 cm^{-1}. We can conclude that the reduced basis functions can be also used for nonrigid molecules to manage memory during high J calculations. In Fig. 6 (right panel), we have plotted the reduced rovibrational energy levels up to $J = 18$ using $p = 12$. The different colours represent the mixing coefficients in the eigenvector decomposition.

D. H_2O_2 molecule

Hydrogen peroxyde is the simplest molecule which undergoes an internal rotation motion. It consists in a torsional motion of the O−H groups around the O−O bond, with a height of

the *trans* barrier ($\rho = \pi$, symmetry point group C_{2h}) around 400 cm^{-1} and of the *cis* barriers ($\rho = 0$, symmetry point group C_{2v}) around 2600 cm^{-1}. Recently, a variational calculation of the energy levels of H_2O_2 was presented in Ref.[147], based on the PES of Malyszek and Koput[148]. It is common to choose the torsion angle between the two "halves" as 2ρ, that is a rotation of $+\rho$ for the first half and of $-\rho$ for the second half (see *e.g.* Refs.[94,149]), whereas a torsional angle of ρ, with rotations of $\pm\rho/2$, was considered in Ref.[150] and in this work. It is important to note that contrary to the three previous molecules, H_2O_2 will pass by *cis* and *trans* configurations with different symmetries as ρ increases from 0 to π; the point group for intermediate configurations being C_2.

If only one barrier is not "insuperable", for example the *trans* barrier, then the permutation-inversion "four-group" G_4 must be used to classify the overall vibration-rotation-torsion energy levels. This group consists of four feasible operations and is isomorphic to the point groups C_{2v} and C_{2h}. But, if the energy splitting due to both the *cis* and *trans* tunnellings can be resolved in observed spectra, as in the case of H_2O_2, Hougen showed that this group must be extended to $G_4(EM)$ in order to properly describe separately the torsional and rotational states. This group is isomorphic to the MS group $D_{2h}(M)$ and to the point group D_{2h} which is already implemented in the TENSOR code. Accordingly, the symmetry species of D_{2h} can be used to classify the energy levels. If we refer now to the reverse correlation table between D_{2h} and C_2, the rigid-molecule A states of C_2 split into A_{1g}, B_{2g}, B_{2u} and A_{1u} components. Alternatively, a quantum number τ taking the values 1, 2, 3 and 4 is generally used to label these four components[94,149].

For hydrogen peroxyde, our energy levels can be directly compared to those computed from the WAVR4 code by Kozin *et al.*[151]. To this end, the *ab initio* PES parameters determined by Malyszek and Koput[148] were used to generate a grid of points that has been fitted using a set of symmetry coordinates in order to be compatible with both TENSOR and WAVR4. Trial calculations were first made using WAVR4 to ensure that the new fitted PES has no hole. The Fortran code as well as the new fitted PES parameters are provided in Supplementary Material. It is worth mentioning at this stage that the aim of the present work was not to reproduce the observed data but to validate the convergence of our Taylor-type expanded hybrid model with respect to the exact KEO model implemented in the WAVR4 computer code. As already shown in Ref.[147], the accuracy of the vibrational band origins using the *ab initio* PES of Malyszek and Koput[148] is within 1 cm^{-1}, but can be

drastically improved using a slightly adjusted PES.

In order to achieve a good convergence, we have studied the dependence of the vibrational levels for the first symmetry block A_g with respect to the truncation order of (i) the kinetic energy operator (8), (ii) the potential (7), (iii) the reduced Hamiltonian (31) and (iv) the basis set (32) For the convergence studies (i), (ii) and (iii), the basis $F(18)$ was employed using the weight coefficients $\kappa_1 = \kappa_5 = 1.2$ and $\kappa_2 = \kappa_6 = 1.1$, $\kappa_3 = \kappa_\rho = 1$.

Convergence study (i). The convergence of the vibrational levels computed with a KEO truncated at order 6, 8 and 10 with respect to that truncated at order 11 is shown in Fig. 7 (top, left panel). This amounts studying the dependence of the energy levels with respect to the $\mu_{\alpha\beta}$ tensor truncation order. For these four calculations, the potential expansion was truncated at order 16. We can see that the levels are converged within 0.001 cm^{-1} (and even below) up to 4000 cm^{-1} using a KEO truncated at order 10.

Convergence study (ii). In Fig. 7 (top, right panel), we give the convergence of the vibrational levels computed with the potential truncated at order 10, 12 and 14 with respect to that truncated at order 16 and by using the 10^{th} order KEO expansion. Similarly to the Watson Hamiltonian[89], we can conclude that the convergence of $\mu_{\alpha\beta}$ is faster than the convergence of V in the HBJ Hamiltonian.

Convergence study (iii). We have also tested the convergence of the reduced (31) and non-reduced (15) Hamiltonian expansion with respect to the non-reduced 16^{th} order Hamiltonian $H(16)$, consisting in a potential truncated at order 16 and a KEO truncated at order 10. We can see in Fig. 7 (bottom, left panel) that the reduced Hamiltonian $H(16 \rightarrow 8)$ is more accurate than the Taylor-based expansion $H(10)$, using less parameters. The reduced Hamiltonian $H(16 \rightarrow 10)$ is converged within 0.001 cm^{-1} up to 3000 cm^{-1} and within 0.01 cm^{-1} up to 4000 cm^{-1} with respect to the full $H(16)$ expansion.

Convergence study (iv). From the Hamiltonian $H(16)$, the convergence of the variational calculation using the basis sets $F(14)$, $F(16)$, $F(18)$ and $F(19)$ with respect to the basis $F(20)$ is displayed in Fig. 7 (bottom, right panel). These basis sets contain 10871, 20961, 37820, 49780 and 64721 vibrational functions of symmetry A_g, respectively. We can see that the $F(16)$ basis would be suitable up to 4000 cm^{-1} for the modelling of low and medium resolution infrared spectra while the $F(19)$ basis allows converging vibrational levels within 0.001 cm^{-1} up to 3500 cm^{-1}.

TABLE I: Comparison of the vibrational band origins of H_2O_2 for the symmetry blocks A_g and B_{1u} obtained from the TENSOR (this work) and WAVR4[151] computer codes. (i) Energy levels (in cm^{-1}) computed with the TENSOR code. The differences WAVR4−TENSOR (in cm^{-1}) are given for different WAVR4 parameters j_{max}, n^a and $icut^b$. We have $(j_{max}, n, icut) = (20, 10, 100)$ in (ii), $(20, 10, 200)$ in (iii), $(20, 10, 300)$ in (iv),$(25, 14, 100)$ in (v), $(25, 14, 200)$ in (vi) and $(25, 14, 300)$ in (vii).

Band	Sym	(i)	(ii)	(iii)	(iv)	(v)	(vi)	(vii)
ν_4	A_g	255.7882	0.0025	0.0019	0.0018	0.0008	0.0002	0.0001
$2\nu_4$	A_g	570.4892	0.0069	0.0043	0.0041	0.0025	−0.0002	−0.0004
ν_3	A_g	865.9407	0.0056	0.0044	0.0044	0.0013	0.0002	0.0001
$3\nu_4$	A_g	1001.7398	0.0087	0.0047	0.0045	0.0034	−0.0007	−0.0008
$\nu_3 + \nu_4$	A_g	1120.4606	0.0075	0.0058	0.0051	0.0026	0.0008	0.0002
ν_6	B_{1u}	1264.3401	0.1387	0.1266	0.1263	0.0132	0.0003	0.0001
ν_2	A_g	1394.5277	0.1271	0.1154	0.1152	0.0128	0.0003	0.0001
$\nu_3 + 2\nu_4$	A_g	1431.7821	0.0199	0.0148	0.0140	0.0057	0.0003	−0.0005
$4\nu_4$	A_g	1478.6183	0.0320	0.0241	0.0240	0.0076	−0.0010	−0.0011
$\nu_4 + \nu_6$	B_{1u}	1505.3746	0.1540	0.1354	0.1351	0.0203	0.0003	0.0001
$\nu_2 + \nu_4$	A_g	1683.5634	0.1592	0.1349	0.1345	0.0269	0.0006	0.0002
$2\nu_3$	A_g	1714.5097	−0.0157	−0.0182	−0.0187	0.0029	0.0005	0.0001
$2\nu_4 + \nu_6$	B_{1u}	1854.0556	0.2180	0.1825	0.1821	0.0364	0.0002	−0.0003
$\nu_3 + 3\nu_4$	A_g	1861.6873	0.0304	0.0214	0.0203	0.0093	−0.0002	−0.0011
$5\nu_4$	A_g	1945.9637	0.0574	0.0299	0.0296	0.0282	−0.0011	−0.0014
$2\nu_3 + \nu_4$	A_g	1967.5418	−0.0269	−0.0317	−0.0329	0.0055	0.0009	−0.0002
$\nu_2 + 2\nu_4$	A_g	1976.1079	0.2358	0.1855	0.1848	0.0561	0.0007	−0.0001
$\nu_3 + \nu_6$	B_{1u}	2113.7491	0.2389	0.2156	0.2148	0.0263	0.0019	0.0011
$\nu_2 + \nu_3$	A_g	2241.9684	0.2514	0.2236	0.2225	0.0317	0.0022	0.0009
$2\nu_3 + 2\nu_4$	A_g	2277.3907	0.0012	−0.0143	−0.0157	0.0150	−0.0005	−0.0018
$3\nu_4 + \nu_6$	B_{1u}	2306.8829	0.3843	0.3169	0.3139	0.0733	0.0028	−0.0007
$6\nu_4$	A_g	2316.7995	0.0758	0.0315	0.0302	0.0463	−0.0003	−0.0017
$\nu_3 + \nu_4 + \nu_6$	B_{1u}	2354.2088	0.2863	0.2430	0.2421	0.0465	0.0016	0.0007

TABLE I – continued

Band	Sym	(i)	(ii)	(iii)	(iv)	(v)	(vi)	(vii)
$\nu_3+4\nu_4$	A_g	2355.9264	0.0609	0.0266	0.0254	0.0354	−0.0006	−0.0018
$\nu_2+3\nu_4$	A_g	2392.7082	0.3737	0.2860	0.2817	0.0958	0.0043	−0.0006
$2\nu_6$	A_g	2505.3506	1.0302	0.9121	0.9043	0.1386	0.0119	0.0030
$\nu_2+\nu_3+\nu_4$	A_g	2530.0509	0.3083	0.2195	0.2176	0.0989	0.0028	0.0009
$3\nu_3$	A_g	2545.5883	−0.6603	−0.6702	−0.6718	0.0030	−0.0021	−0.0027
$\nu_2+\nu_6$	B_{1u}	2648.8057	1.8124	1.6103	1.5977	0.2427	0.0202	0.0061
$\nu_3+2\nu_4+\nu_6$	B_{1u}	2701.2782	0.3994	0.2994	0.2979	0.1012	0.0008	−0.0008
$2\nu_3+3\nu_4$	A_g	2705.2429	0.0315	−0.0012	−0.0030	0.0301	−0.0037	−0.0054
$7\nu_4$	A_g	2720.3876	0.1485	0.0579	0.0549	0.0964	−0.0011	−0.0043
$\nu_4+2\nu_6$	A_g	2743.9942	1.4453	1.1785	1.1665	0.3147	0.0169	0.0040
$2\nu_2$	A_g	2765.5520	1.0040	0.7899	0.7788	0.2444	0.0153	0.0028
$3\nu_3+\nu_4$	A_g	2796.6891	−0.6625	−0.6821	−0.6856	0.0051	−0.0066	−0.0082
$4\nu_4+\nu_6$	B_{1u}	2799.9239	0.5421	0.2867	0.2796	0.3039	0.0054	−0.0022
$\nu_3+5\nu_4$	A_g	2809.5394	0.2537	0.1122	0.1106	0.1563	−0.0011	−0.0029
$\nu_2+\nu_3+2\nu_4$	A_g	2824.6633	0.3854	0.1918	0.1894	0.2082	0.0012	−0.0016
$\nu_2+4\nu_4$	A_g	2861.3768	0.6177	0.2763	0.2684	0.3969	0.0066	−0.0017
$\nu_2+\nu_4+\nu_6$	B_{1u}	2914.7957	2.6087	1.8111	1.7898	0.8872	0.0279	0.0072
$2\nu_3+\nu_6$	B_{1u}	2945.3719	0.2881	0.2364	0.2341	0.0554	0.0018	0.0000
rms error			0.6452	0.5064	0.5018	0.1851	0.0071	0.0026

[a] j_{max} and n are the numbers of angular and radial functions (see Ref.[151]).

[b] *icut* is the number of selected eigenvectors at each step (see Ref.[151]).

TABLE II: Comparison of the vibrational band origins of H_2O_2 for the symmetry blocks A_u and B_{1g} obtained with the TENSOR (this work) and WAVR4 computer codes. See caption of Tab. I for the definition of the different columns.

Band	Sym	(i)	(ii)	(iii)	(iv)	(v)	(vi)	(vii)
GS	A_u	11.2122	-0.0034	-0.0034	0.0033	-0.0003	0.0000	-0.0001
ν_4	A_u	371.3261	−0.0014	−0.0015	0.0015	−0.0001	−0.0001	−0.0002

TABLE II – continued

Band	Sym	(i)	(ii)	(iii)	(iv)	(v)	(vi)	(vii)
$2\nu_4$	A_u	776.8274	0.0119	0.0103	−0.0101	0.0014	−0.0018	−0.0006
ν_3	A_u	877.6885	0.0087	0.0077	−0.0078	0.0010	−0.0011	0.0000
$\nu_3 + \nu_4$	A_u	1227.0708	0.0134	0.0112	−0.0109	0.0020	−0.0022	−0.0005
$3\nu_4$	A_u	1245.4558	0.0155	0.0131	−0.0128	0.0023	−0.0025	−0.0006
ν_6	B_{1g}	1284.6829	0.1640	0.1548	−0.1546	0.0099	−0.0097	0.0000
ν_2	A_u	1400.7098	0.1674	0.1574	−0.1571	0.0107	−0.0104	0.0000
$\nu_3 + 2\nu_4$	A_u	1638.1640	0.0202	0.0170	−0.0162	0.0039	−0.0038	−0.0007
$\nu_4 + \nu_6$	B_{1g}	1648.4799	0.2196	0.2066	−0.2064	0.0138	−0.0136	0.0001
$4\nu_4$	A_u	1720.1736	0.0330	0.0261	−0.0260	0.0066	−0.0077	−0.0011
$3\nu_3$	A_u	1726.8764	−0.0076	−0.0101	0.0102	0.0025	−0.0025	0.0000
$\nu_2 + \nu_3$	A_u	1772.8478	0.2064	0.1894	−0.1891	0.0181	−0.0178	0.0000
$2\nu_4 + \nu_6$	B_{1g}	2072.6916	0.2268	0.2033	−0.2030	0.0269	−0.0269	−0.0004
$2\nu_3 + \nu_4$	A_u	2076.4227	0.0016	−0.0028	0.0034	0.0044	−0.0043	−0.0005
$\nu_3 + 3\nu_4$	A_u	2103.3759	0.0231	0.0160	−0.0152	0.0072	−0.0075	−0.0010
$\nu_3 + \nu_6$	B_{1g}	2134.6189	0.2206	0.2036	−0.2025	0.0193	−0.0178	0.0005
$\nu_2 + 2\nu_4$	A_u	2170.7709	0.2092	0.1735	−0.1730	0.0400	−0.0398	−0.0004
$5\nu_4$	A_u	2205.8643	0.0567	0.0305	−0.0303	0.0267	−0.0280	−0.0014
$\nu_2 + \nu_3$	A_u	2248.5455	0.2091	0.1873	−0.1864	0.0246	−0.0230	0.0008
$2\nu_3 + 2\nu_4$	A_u	2483.5870	−0.0086	−0.0154	0.0168	0.0074	−0.0076	−0.0015
$\nu_3 + \nu_4 + \nu_6$	B_{1g}	2496.0545	0.2672	0.2396	−0.2389	0.0297	−0.0282	0.0008
$2\nu_6$	A_u	2538.4081	0.9592	0.8801	−0.8778	0.0921	−0.0864	0.0027
$3\nu_4 + \nu_6$	B_{1g}	2551.8234	0.3660	0.3021	−0.2999	0.0689	−0.0670	−0.0006
$3\nu_3$	A_u	2558.3483	−0.6483	−0.6569	0.6582	0.0035	−0.0048	−0.0015
$\nu_3 + 4\nu_4$	A_u	2579.2230	0.0632	0.0440	−0.0435	0.0193	−0.0201	−0.0012
$\nu_2 + \nu_3 + \nu_4$	A_u	2614.6564	0.3396	0.2791	−0.2773	0.0658	−0.0633	0.0005
$\nu_2 + 3\nu_4$	A_u	2628.8437	0.3410	0.2729	−0.2703	0.0741	−0.0713	−0.0001
$\nu_2 + \nu_6$	B_{1g}	2660.3104	1.4349	1.3261	−1.3199	0.1318	−0.1203	0.0045
$6\nu_4$	A_u	2705.4012	0.1297	0.0716	−0.0697	0.0603	−0.0604	−0.0023

TABLE II – continued

Band	Sym	(i)	(ii)	(iii)	(iv)	(v)	(vi)	(vii)
$2\nu_2$	A_u	2768.9855	0.8934	0.7426	−0.7364	0.1715	−0.1623	0.0022
$3\nu_2+\nu_4$	A_u	2908.1590	−0.5381	−0.5535	0.5561	0.0049	−0.0089	−0.0050
$\nu_4+2\nu_6$	A_u	2910.8426	1.1266	0.9862	−0.9787	0.1694	−0.1578	0.0027
$\nu_3+2\nu_4+\nu_6$	B_{1g}	2918.9996	0.4153	0.3473	−0.3461	0.0781	−0.0770	−0.0001
$2\nu_3+3\nu_4$	A_u	2945.9496	−0.0863	−0.1090	0.1109	0.0182	−0.0222	−0.0053
$2\nu_3+\nu_6$	B_{1g}	2966.8810	0.2657	0.2261	−0.2239	0.0418	−0.0398	0.0001
rms error			0.4347	0.3932	0.3915	0.0569	0.0539	0.0018

Finally, we give in Tabs. I and II the differences between the vibrational energy levels computed from the TENSOR and WAVR4[151] computer codes for the symmetry blocks (A_g, B_{1u}) and (A_u, B_{1g}), respectively. We can see that the results obtained from WAVR4 are quite sensitive to the input parameters $(j_{max}, n, icut)$ (see Ref.[151] for more explanations), in particular for converging the overtones of the torsional mode ν_4. Several days of calculation were necessary to compute the $J=0$ levels using WAVR4 for $(j_{max}, n, icut) = (25, 14, 300)$ against few hours using TENSOR. Finally, we can note the very good agreement between both calculations, with errors ~ 0.001 cm^{-1} up to 3000 cm^{-1}, which is much better than the agreement between TROVE and WAVR4 in Ref.[147], with deviations up to 0.5 cm^{-1}.

V. CONCLUSION

In this paper, we have proposed an hybrid nuclear-motion Hamiltonian based on the HBJ formalism but written in terms of ITOs adapted to a given molecular symmetry group. The treatment of the nonrigid coordinate is made numerically on a grid of points suitably chosen in order to accelerate the computation of the energy levels. For each point of the grid, a set of vibrational-rotational ITOs is constructed. In the introduction part, we asked a question about the pertinence of using the tools which were developed for semirigid molecules. We can answer positively to this question. Indeed, we have shown that the ITO formalism initially introduced in the construction of effective Hamiltonian for semirigid spherical top molecules as well as the Hamiltonian and basis-set reduction procedure introduced to accelerate calculations are also both designed to nonrigid molecules. The hybrid model has

been validated on small nonrigid systems (CH_2, CH_3, NH_3, H_2O_2) and will pave the way for the study of more complex molecules, with possibly several large amplitude motions, for the analysis of high-resolution spectra and for the construction of molecular line lists.

Undoubtedly, the construction of nonrigid effective models, as proposed in Ref.[90], would be of great help to refine parameters quite easily on observed data. Moreover, an upcoming version of TENSOR is in preparation and will benefit from the use of iterative eigensolvers and nested contracted basis functions in conjunction with group-theoretical considerations in order to consider molecules with more than 7 atoms, as ethane-like molecules.

SUPPLEMENTARY MATERIAL

Fortran code including the H_2O_2 PES in symmetry coordinates used in this work and generated from the *ab initio* PES by Malyszek and Koput[148].

ACKNOWLEDGMENTS

The authors acknowledge support from the Romeo computer center of Reims-Champagne-Ardenne, from the program IRP "SAMIA2", and from the French ANR TEMMEX project (Grant 21-CE30-0053-01). This work was supported by the Russian Scientific Foundation (RSF, No. 22-42-09022). This work is dedicated to Professor Per Jensen who is gratefully acknowledged for the fruitful discussions he shared with the authors during his visit in Reims.

AUTHOR DECLARATIONS

Conflict of interest

The authors have no conflicts to disclose

Appendix A: Derivation of the rotation matrix $\mathbf{U}(\rho)$ in Eq. (1)

Szalay and Ortigoso[152] already derived the rotation matrix $\mathbf{U}(\rho)$ involved in Eq. (1) using the Floquet theory[153]. More recently, an alternative method was proposed in Ref.[93]

and consists in integrating the evolution equation

$$\frac{d\mathbf{U}(\rho)}{d\rho} = \mathbf{U}(\rho)\mathbf{\Omega}(\rho), \tag{A1}$$

using the elements of the Lie group SO(3) and Lie algebra so(3). In Eq. (A1), $\mathbf{\Omega}(\rho)$ is a skew-symmetric matrix involving the LAM dependent angular velocity vector components $(\omega_x, \omega_y, \omega_z)$ defined by $\boldsymbol{\omega}(\rho) = -(\mathbf{I}_{\text{Rot-Rot}})^{-1}\mathbf{I}_{\text{Rot-LAM}}$ where $\mathbf{I}_{\text{Rot-Rot}}(\rho)$ is the rotational tensor of inertia. Introducing the three generators of the so(3) Lie algebra

$$\begin{gathered} S_x = \begin{pmatrix} 0 & 0 & 0 \\ 0 & 0 & -1 \\ 0 & 1 & 0 \end{pmatrix} \quad , \quad S_y = \begin{pmatrix} 0 & 0 & 1 \\ 0 & 0 & 0 \\ -1 & 0 & 0 \end{pmatrix} \\ \text{and} \quad S_z = \begin{pmatrix} 0 & -1 & 0 \\ 1 & 0 & 0 \\ 0 & 0 & 0 \end{pmatrix}, \end{gathered} \tag{A2}$$

the elements of the SO(3) rotation Lie group can be obtained *via* the exponential map

$$\mathbf{U}(\rho) = e^{\mathbf{P}(\rho)}, \tag{A3}$$

with $\mathbf{P}(\rho) = \sum \mathfrak{p}_\alpha(\rho) S_\alpha$ ($\alpha = x$, y and z). Here, the three components $\mathfrak{p}_x(\rho)$, $\mathfrak{p}_y(\rho)$ and $\mathfrak{p}_z(\rho)$ are to be determined. Similarly, we can write $\mathbf{\Omega}(\rho) = \sum \omega_\alpha(\rho) S_\alpha$. After some algebra, we can show that

$$\frac{d\mathbf{P}}{d\rho} = \boldsymbol{\omega} \ \cdot \mathbf{S} + \mathbf{T} \cdot \mathbf{S}, \tag{A4}$$

where we have defined

$$T_\alpha = \sum_{r=1}^{\infty} (-1)^r (\boldsymbol{\mathfrak{p}} \cdot \boldsymbol{\mathfrak{p}})^{r-1} \left\{ \left[(\boldsymbol{\mathfrak{p}} \cdot \boldsymbol{\mathfrak{p}}) \omega_\alpha - (\boldsymbol{\mathfrak{p}} \cdot \boldsymbol{\omega}) \mathfrak{p}_\alpha \right] \frac{B_{2r}}{(2r)!} + (\boldsymbol{\mathfrak{p}} \times \boldsymbol{\omega})_\alpha \frac{B_{2r-1}}{(2r-1)!} \right\}, \tag{A5}$$

with B_k the Bernoulli numbers. Bearing in mind that the only non-vanishing term B_{2r-1} is given for $r = 1$ and using the expansion in Laurent series of $\cot(z)$ around $z = 0$, the elements p_α are determined by solving a system of three ordinary differential equations

$$\mathfrak{p}'_\alpha(\rho) = \frac{1}{2}(\boldsymbol{\mathfrak{p}} \times \boldsymbol{\omega})_\alpha + \frac{\omega_\alpha}{2} \left\| \mathfrak{p} \right\| \cot\left(\frac{\left\| \mathfrak{p} \right\|}{2} \right) - \frac{(\boldsymbol{\mathfrak{p}} \cdot \boldsymbol{\omega}) \mathfrak{p}_\alpha}{2 \left\| \mathfrak{p} \right\|^2} \left[\left\| \mathfrak{p} \right\| \cot\left(\frac{\left\| \mathfrak{p} \right\|}{2} \right) - 2 \right]. \tag{A6}$$

Finally, by employing the Rodrigues formula one calculate easily the desired rotation matrix (A3). Alternatively, the exponential in (A3) can be disentangled as $\mathbf{U}(\rho) = e^{\mathfrak{g}_x S_x} e^{\mathfrak{g}_y S_y} e^{\mathfrak{g}_z S_z}$

where the elements $\mathfrak{g}_\alpha$ can be related to the p_α's as

$$\begin{aligned} \mathfrak{g}_x &= \arcsin\left(-\frac{w}{\sqrt{1-v^2}}\right), \\ \mathfrak{g}_y &= \arcsin(v), \\ \mathfrak{g}_z &= \arcsin\left(-\frac{u}{\sqrt{1-v^2}}\right), \end{aligned} \tag{A7}$$

with

$$\begin{aligned} u &= -\frac{\mathfrak{p}_z}{\|\mathfrak{p}\|}\sin(\|\mathfrak{p}\|) + \frac{\mathfrak{p}_x\mathfrak{p}_y}{\|\mathfrak{p}\|^2}(1-\cos(\|\mathfrak{p}\|)), \\ v &= \frac{\mathfrak{p}_y}{\|\mathfrak{p}\|}\sin(\|\mathfrak{p}\|) + \frac{\mathfrak{p}_x\mathfrak{p}_z}{\|\mathfrak{p}\|^2}(1-\cos(\|\mathfrak{p}\|)), \\ w &= -\frac{\mathfrak{p}_x}{\|\mathfrak{p}\|}\sin(\|\mathfrak{p}\|) + \frac{\mathfrak{p}_y\mathfrak{p}_z}{\|\mathfrak{p}\|^2}(1-\cos(\|\mathfrak{p}\|)). \end{aligned} \tag{A8}$$

In order to make the link with the Hougen's paper[71], we could also introduce the Euler angles as

$$\begin{aligned} \theta &= \arccos\left[\cos(\mathfrak{g}_x)\cos(\mathfrak{g}_y)\right], \\ \phi &= \arccos\left[\frac{\sin(\mathfrak{g}_y)}{\sqrt{1-\cos^2(\mathfrak{g}_x)\cos^2(\mathfrak{g}_y)}}\right], \\ \psi &= \arccos\left[\frac{\cos(\mathfrak{g}_x)\sin(\mathfrak{g}_y)\cos(\mathfrak{g}_z)-\sin(\mathfrak{g}_x)\sin(\mathfrak{g}_z)}{\sqrt{1-\cos^2(\mathfrak{g}_x)\cos^2(\mathfrak{g}_y)}}\right]. \end{aligned} \tag{A9}$$

REFERENCES

[1]P. F. Bernath, Phil. Trans. R. Soc. A **372**, 20130087 (2014).

[2]J. Tennyson, S. N. Yurchenko, A. F. Al-Refaie, V. H. J. Clark, K. L. Chubb, *et al.*, J. Quant. Spectrosc. Radiat. Transf. **255**, 107228 (2020).

[3]M. R. Aliev and J. K. G. Watson, *Higher-order effects in the vibration-rotation spectra of semirigid molecules*, edited by K. N. Rao (Academic Press, London, 1985).

[4]D. Papousek and M. R. Aliev, *Molecular vibrational-rotational spectra* (Elsevier Scientific Publishing Company, Amsterdam-Oxford-New York, 1982).

[5]J. K. G. Watson, Mol. Phys. **103**, 3283 (2005).

[6]I. Kleiner, J. Mol. Spectrosc. **260**, 1 (2010).

[7]J. M. Bowman, X. Huang, N. C. Handy, and S. Carter, J. Phys. Chem. A **111**, 7317 (2007).

[8]S. N. Yurchenko, W. Thiel, and P. Jensen, J. Mol. Spectrosc. **245**, 126 (2007).

[9]E. Mátyus, J. Šimunek, and A. G. Császár, J. Chem. Phys. **131**, 074106 (2009).

[10]P. Cassam-Chenaï and J. Liévin, J. Mol. Spectrosc. **291**, 77 (2013).

[11]A. Owens, S. N. Yurchenko, A. Yachmenev, J. Tennyson, and W. Thiel, J. Chem. Phys. **145**, 104305 (2016).

[12]A. V. Nikitin, M. Rey, and V. G. Tyuterev, J. Quant. Spectrosc. Radiat. Transfer **200**, 90 (2017).

[13]M. Rey, I. S. Chizhmakova, A. V. Nikitin, and V. G. Tyuterev, Phys. Chem. Chem. Phys. **20**, 21008 (2018).

[14]D. Bégué, N. Gohaud, C. Pouchan, P. Cassam-Chenai, and J. Liévin, J. Chem. Phys. **127**, 164115 (2007).

[15]C. Fábri, E. Mátyus, T. Furtenbacher, L. Nemes, B. Mihály, T. Zoltáni, and A. Császár, J. Chem. Phys. **135**, 094307 (2011).

[16]S. Carter, A. Sharma, and J. Bowman, J. Chem. Phys. **137**, 15 (2012).

[17]X.-G. Wang and J. Carrington, T., J. Chem. Phys. **144**, 204304 (2016).

[18]P. Thomas and J. Carrington, T., J. Chem. Phys. **146**, 204110 (2017).

[19]C. Fábri, M. Quack, and A. G. Császár, J. Chem. Phys. **147**, 134101 (2017).

[20]G. Mulas, C. Falvo, P. Cassam-Chenaï, and C. Joblin, J. Chem. Phys. **149**, 144102 (2018).

[21]M. Rey, I. S. Chizhmakova, A. V. Nikitin, and V. G. Tyuterev, Phys. Chem. Chem. Phys. **23**, 12115 (2021).

[22]T. Mathea, T. Petrenko, and G. Rauhut, J. Phys. Chem. A **125**, 990 (2021).

[23]M. Tschöpe, B. Schröder, S. Erfort, and G. Rauhut, Frontiers in Chemistry **8**, 623641 (2021).

[24]P. Cassam-Chenaï and J. Liévin, J. Comp. Chem. **27**, 627 (2006).

[25]R. Garnier, M. Odunlami, V. Le Bris, D. Bégué, I. Baraille, and O. Coulaud, J. Chem. Phys. **144**, 204123 (2016).

[26]A. Leclerc and T. Carrington, Jr., Chem. Phys. Letters **644**, 183 (2016).

[27]M. Odunlami, V. Le Bris, D. Bégué, I. Baraille, and O. Coulaud, J. Chem. Phys. **146**, 214108 (2017).

[28]T. Petrenko and G. Rauhut, J. Chem. Phys. **146**, 124101 (2017).

[29]G. Avila and J. Carrington, T., J. Chem. Phys. **147**, 064103 (2017).

[30]S. Manzhos, X. Wang, and J. Carrington, T., Chem. Phys. **509**, 139 (2018).

[31]R. Wodraszka and J. Carrington, T., J. Chem. Phys. **150**, 154108 (2019).

[32]E. Zak and J. Carrington, T., J. Chem. Phys. **150**, 204108 (2019).

[33]S. Erfort, M. Tschöpe, and G. Rauhut, J. Chem. Phys. **152**, 244104 (2020).

[34]J. Carrington, T., Spectrochimica Acta - Part A **248**, 119158 (2021).

[35]B. Schröder and G. Rauhut, J. Chem. Phys. **154**, 124114 (2021).

[36]N. Handy, Mol. Phys. **61**, 207 (1987).

[37]R. Islampour and S. Lin, J. Mol. Spectrosc. **147**, 1 (1991).

[38]X. Chapuisat and C. Iung, Phys. Rev. A **45**, 6217 (1992).

[39]A. Császár and N. Handy, The J. Chem. Phys. **102**, 3962 (1995).

[40]F. Gatti and C. Iung, Phys. Rep. **484**, 1 (2009).

[41]J. Frederick and C. Woywod, J. Chem. Phys. **111**, 7255 (1999).

[42]J. Makarewicz and A. Skalozub, Chem. Phys. Letters **306**, 352 (1999).

[43]M. Mladenovic, J. Chem. Phys. **112**, 1070 (2000).

[44]J. Pesonen, J. Chem. Phys. **128** (2008), 10.1063/1.2829496.

[45]K. Sadri, D. Lauvergnat, F. Gatti, and H. D. Meyer, J. Chem. Phys. **136**, 234112 (2012).

[46]X.-G. Wang and T. Carrington, Jr., J. Chem. Phys. **138**, 104106 (2013).

[47]C. Fábri, E. Mátyus, and A. G. Császár, Spectrochimica A **119**, 84 (2014).

[48]A. E. Protasevich and A. V. Nikitin, J. Chem. Phys. **116**, 44 (2018).

[49]W. A. Kopp and K. Leonhard, J. Chem. Phys. **145**, 234102 (2016).

[50]J. K. G. Watson, Mol. Phys. **15**, 479 (1968).

[51]M. Rey, T. Delahaye, A. V. Nikitin, and V. G. Tyuterev, A&A **594**, A47 (2016).

[52]M. Rey, A. V. Nikitin, B. Bézard, P. Rannou, A. Coustenis, and V. G. Tyuterev, Icarus **303**, 114 (2018).

[53]M. Rey, A. V. Nikitin, and V. G. Tyuterev, ApJ **847**, 1 (2017).

[54]M. Schneider and G. Rauhut, J. Comp. Chem. **44**, 298 (2023).

[55]M. Tschöpe and G. Rauhut, Ap J. **949** (2023).

[56]P. Jensen, J. Mol. Spectrosc. **128**, 478 (1988).

[57]S. Yurchenko, W. Thiel, M. Carvajal, H. Lin, and P. Jensen, Adv. Quant. Chem. **48**, 14 (2005).

[58]X. Huang, D. W. Schwenke, and T. J. Lee, J. Chem. Phys. **134**, 044321 (2011).

[59]D. Lauvergnat and A. Nauts, Phys. Chem. Chem. Phys. **12**, 8405 (2010).

[60]D. Lauvergnat, J. M. Luis, B. Kirtman, H. Reis, and A. Nauts, J. Chem. Phys. **144**, 084116 (2016).

[61]A. Nauts and D. Lauvergnat, Mol. Phys. **116**, 3701 (2018).

[62]L. H. Coudert and J. T. Hougen, J. Mol. Spectrosc. **149**, 73 (1991).

[63]H. Nguyen, I. Gulaczyk, M. Kreglewski, and I. Kleiner, Coord. Chemistry Reviews **436** (2021).

[64]H. V. L. Nguyen and I. Kleiner, Phys. Sciences Rev. **7**, 679 (2022).

[65]I. Gulaczyk and M. Kreglewski, Phys. Sciences Reviews **8**, 259 (2023).

[66]H. C. Longuet-Higgins, Mol. Phys. **6**, 445 (1963).

[67]C. M. Woodman, Mol. Phys. **19**, 753 (1970).

[68]J. K. G. Watson, Can. J. Phys. **43.**, 1996 (1965).

[69]Y. G. Smeyers, Adv. Quantum Chem. **24**, 1 (1992).

[70]N. Ohashi and J. T. Hougen, J. Mol. Spectrosc. **163**, 86 (1994).

[71]J. T. Hougen, J. Mol. Spectrosc. **181**, 287 (1997).

[72]T. Mellor, S. Yurchenko, B. Mant, and P. Jensen, Symmetry **11** (2019).

[73]J. T. Hougen, J. Phys. Chem. **90**, 562 (1986).

[74]P. R. Bunker and P. Jensen, *Molecular Symmetry and Spectroscopy* (NRC-CNRC, Ottawa, 1998).

[75]J. T. Hougen, P. R. Bunker, and J. W. C. Johns, J. Mol. Spectrosc. **34**, 136 (1970).

[76]V. Szalay, J. Mol. Spectrosc. **102**, 13 (1983).

[77]K. Sarka, J. Mol. Spectrosc. **38**, 545 (1971).

[78]D. C. Moule and C. V. S. Ramachandra Rao, J. Mol. Spectrosc. **45**, 120 (1973).

[79]G. Dellepiane, M. Gussoni, and J. T. Hougen, J. Mol. Spectrosc. **47**, 515 (1973).

[80]D. Papousek, V. Spirko, S. Urban, J. Kauppinen, A. F. Krupnov, and K. Narahari Rao, J. Mol. Struc. **80**, 1 (1982).

[81]P. Jensen, Computer Physics Reports **1**, 1 (1983).

[82]P. Jensen and P. R. Bunker, J. Mol. Spectrosc. **99**, 348 (1983).

[83]R. Beardsworth, P. R. Bunker, P. Jensen, and W. P. Kraemer, J. Mol. Spectrosc. **118**, 50 (1986).

[84]K. Sarka and H. W. Schrotter, J. Mol. Spectrosc. **179**, 195 (1996).

[85]V. V. Ilyushin, Z. Kisiel, L. Pszczólkowski, H. Mäder, and J. T. Hougen, J. Mol. Spectrosc. **259**, 26 (2010).

[86]I. Kleiner and J. T. Hougen, J. Phys. Chem. A **119**, 10664 (2015).

[87]D. Viglaska, M. Rey, A. V. Nikitin, and V. G. Tyuterev, J. Chem. Phys. **153**, 084102 (2020).

[88]M. Rey, A. V. Nikitin, and V. G. Tyuterev, J. Chem. Phys. **136**, 244106 (2012).

[89]M. Rey, A. Nikitin, and V. Tyuterev, J. Quant. Spectrosc. Radiat. Transf. **164**, 207 (2015).

[90]M. Rey, J. Chem. Phys. **156** (2022).

[91]D. Papousek, *Vibration-Rotational Spectroscopy and Molecular Dynamic−Advances in Quantum Chemical and Spectroscopical Studies of Molecular Structures and Dynamics* (Advanced series in physical chemistry, volume 9, 1997) pp. 396–460.

[92]D. Papousek, J. Mol. Struc. **100**, 179 (1983).

[93]V. Szalay, D. Viglaska, and M. Rey, J. Chem. Phys. **149**, 244118 (2018).

[94]J.-M. Flaud, C. Camy-Peyret, J. W. C. Johns, and B. Carli, J. Chem. Phys. **91**, 1504 (1989).

[95]A. Sayvetz, J. Chem. Phys. **7**, 383 (1939).

[96]V. Szalay, J. Mol. Spectrosc. **128**, 24 (1988).

[97]V. Szalay, J. Chem. Phys. **140** (2014).

[98]M. Rey, J. Chem. Phys. **151**, 024101 (2019).

[99]A. R. Hoy, I. M. Mills, and G. Strey, Mol. Phys. **24**, 1265 (1972).

[100]H. Hartwig and H. Dreizler, Zeitschrift fur Naturforschung **51**, 923 (1996).

[101]I. Kleiner and J. T. Hougen, J. Chem. Phys. **119**, 5505 (2003).

[102]J. T. Hougen, I. Kleiner, and M. Godefroid, J. Mol. Spectrosc. **163**, 559 (1994).

[103]M. Tudorie, I. Kleiner, J. T. Hougen, S. Melandri, L. W. Sutikdja, and W. Stahl, J. Mol. Spectrosc. **269**, 211 (2011).

[104]P. Groner, J. Chem. Phys. **107**, 4483 (1997).

[105]K. Makino and M. Berz, Nucl. Instrum. Methods Phys. Res. A **558**, 346 – 350 (2006).

[106]P. Soldán, J. Mol. Spectrosc. **180**, 249 (1996).

[107]P. R. Bunker and P. Jensen, *Fundamentals of Molecular Symmetry* (IOP Publishing, Bristol and Philadelphia, 2006).

[108]P. Groner, J. Mol. Spectrosc. **343**, 34 (2018).

[109]J. T. Hougen, J. Mol. Spectrosc. **256**, 170 (2009).

[110]Y. G. Smeyers and M. Villa, J. Math. Chem. **28**, 377 (2000).

[111]W. G. Harter, *Principles of Symmetry, Dynamics, and Spectroscopy* (John Wiley & Sons, University of Arkansas, Fayetteville, Arkansas, 1993).

[112]J. P. Champion, M. Loëte, and G. Pierre, *Spherical Top Spectra* (Academic Press, K N Rao A Weber, San Diago, 1992).

[113]V. N. Saveliev and O. N. Ulenikov, J. Phys. B: Atomic and Molecular Physics **20**, 67 (1987).

[114]C. Roche, J.-P. Champion, S. Coy, J. Klaassen, J. Steinfeld, A. Valentin, Y. Mizugai, and J. Johns, J. Chem. Phys. **100**, 5508 – 5518 (1994).

[115]A. V. Nikitin, J. P. Champion, and V. G. Tyuterev, J. Mol. Spectrosc. **182**, 72 (1997).

[116]V. Boudon, J. P. Champion, T. Gabard, M. Loëte, F. Michelot, G. Pierre, M. Rotger, C. Wenger, and M. Rey, J. Mol. Spectrosc. **228**, 620 (2004).

[117]J. Moret-Bailly, J. Mol. Spectrosc. **50**, 483 – 484 (1974).

[118]F. Michelot, J. Moret-Bailly, and K. Fox, J. Chem. Phys. **60**, 2610 – 2616 (1974).

[119]F. Michelot, J. Moret-Bailly, and K. Fox, J. Chem. Phys. **60**, 2606 – 2609 (1974).

[120]B. Zhilinskii, Opt. Spectrosc. **51**, 262 (1981).

[121]V. Boujut and F. Michelot, J. Mol. Spectrosc. **173**, 237 (1995).

[122]F. Michelot, M. Rey, and V. Boudon, J. Mol. Spectrosc. **220**, 19 (2003).

[123]F. Michelot and M. Rey, Eur. Phys. J. D **30**, 181 (2004).

[124]F. Michelot and M. Rey, Eur. Phys. J. D **33**, 357 (2005).

[125]M. Rey, V. Boudon, M. Loëte, and F. Michelot, J. Mol. Spectrosc. **204**, 106 (2000).

[126]M. Rey, V. Boudon, and M. Loëte, J. Mol. Struct. **599**, 125 (2001).

[127]M. Rey, "Vibrational and rotational irreductible tensor operators for Abelian and non-Abelian symmetry groups" (unpublished).

[128]M. Rey, V. Boudon, C. Wenger, G. Pierre, and B. Sartakov, J. Mol. Spectrosc. **219**, 313 (2003).

[129]S. Altmann and F. Palacio, Mol. Phys. **38**, 513 (1979).

[130]E. P. Wigner, *Group theory and its applications to the quantum mechanics of atomic spectra* (Academic press, Princeton, New Jersey, 1959).

[131]O. Egorov, M. Rey, A. V. Nikitin, and D. Viglaska, J. Phys. Chem. A **125**, 10568 (2021).

[132]O. Egorov, M. Rey, A. V. Nikitin, and D. Viglaska, J. Phys. Chem. A **126**, 6429 – 6442 (2022).

[133]O. Egorov, M. Rey, A. V. Nikitin, and D. Viglaska, submitted (2023).

[134]M. Tschöpe and G. Rauhut, J. Chem. Phys. **157**, 234105 (2022).

[135]J. Tennyson, M. A. Kostin, P. Barletta, G. Harris, O. L. Polyansky, J. Ramanlal, and N. F. Zobov, Comp. Phys. Comm. **163**, 85 (2004).

[136]A. D. McLean, P. R. Bunker, R. M. Escribano, and P. Jensen, J. Chem. Phys. **87**, 2166 (1987).

[137]P. R. Bunker, P. Jensen, W. P. Kraemer, and R. Beardsworth, J. Chem. Phys. **85**, 3724 (1986).

[138]P. Jensen, P. Bunker, and A. R. Hoy, J. Chem. Phys. **77**, 5370 (1982).

[139]T. Furtenbacher, G. Czakó, B. Sutcliffe, A. G. Császár, and V. Szalay, J. Mol. Struc. **780-781**, 283 (2006).

[140]L. H. Coudert, J. Chem. Phys. **153** (2020).

[141]J. Louck and W. Shaffer, J. Mol. Spectrosc. **4**, 285 (1960).

[142]A. Y. Adam, A. Yachmenev, S. N. Yurchenko, and P. Jensen, J. Phys. Chem. A **123**, 4755 (2019).

[143]S. Yurchenko, R. Barber, and J. Tennyson, Month. Notices Royal Astro. Society **413**, 1828 – 1834 (2011).

[144]A. R. Al Derzi, T. Furtenbacher, J. Tennyson, S. N. Yurchenko, and A. G. Császár, J. Quant. Spectrosc. Radiat. Transf. **161**, 117 – 130 (2015).

[145]M. Rey, F. Michelot, and V. G. Tyuterev, Phys. Rev. A **78**, 022511 (2008).

[146]F. De Oliveira, M. Kim, P. Knight, and V. Buek, Phys. Rev. A **41**, 2645 – 2652 (1990).

[147]O. L. Polyansky, I. N. Kozin, R. I. Ovsyannikov, P. Malyszek, J. Koput, J. Tennyson, and S. N. Yurchenko, J. Phys. Chem. A **117**, 7367 (2013).

[148]P. Malyszek and J. Koput, J. Comp. Chem. **34**, 337 (2013).

[149]J. T. Hougen, Can. J. Phys. **62**, 1392 (1984).

[150]R. H. Hunt, R. A. Leacock, C. Wilbur P., and K. T. Hecht, J. Chem. Phys. **42**, 1931 (1965).

[151]I. N. Kozin, M. M. Law, J. Tennyson, and J. M. Hutson, Comp. Phys. Commu. **163**, 117 (2004).

[152]V. Szalay and J. Ortigoso, J. Chem. Phys. **109**, 3911 (1998).

[153]J. Shirley, Phys. Rev. B. **138**, 979 (1965).